To the Graduate Council:

I am submitting herewith a thesis written by John Michael Sebghati entitled "Monitoring Axial Flow Compressors for Rotating Stall and Surge." I have examined the final copy of this thesis for form and content and recommend that it be accepted in partial fulfillment of the requirements for the degree of Master of Science, with a major in Aerospace Engineering.

Ching F. Lo, Major Professor

We have read this thesis
and recommend its acceptance:

Charles C. Limbaugh

Roy J. Schulz

Accepted for the Council:

CWMinkel

Associate Vice Chancellor
and Dean of The Graduate School

STATEMENT OF PERMISSION TO USE

In presenting this thesis in partial fulfillment of the requirement for a Master's degree at The University of Tennessee, Knoxville, I agree that the Library shall make it available to borrowers under rules of the Library. Brief quotations from this thesis are allowable without special permission, provided that accurate acknowledgment of the source is made.

Permission for extensive quotation from or reproduction of this thesis may be granted by my major professor, or in his absence, by Head of Interlibrary Services when, in the opinion of either, the proposed use of the material is for scholarly purposes. Any copying or use of the material in this thesis for financial gain shall not be allowed without my permission.

Signature John M. Selvaggi

Date 4/30/92

MONITORING AXIAL-FLOW COMPRESSORS FOR ROTATING STALL AND SURGE

A Thesis

Presented for the

Master of Science

Degree

The University of Tennessee, Knoxville

John Michael Sebghati

May 1992

ABSTRACT

The rapid detection of flow instabilities like rotating stall and surge is of paramount importance in operating axial-flow compressors safely and efficiently. Monitoring these phenomena before they have reached full strength is difficult, and requires watching the axial-flow compressor in great detail.

A number of measurement methods exist which can aid in this detection: they include, hot-wire anemometers, thermocouples, pressure transducers, strain gages, optical sensors, and acoustical sensors. Research is currently under way on using high response static pressure transducers to detect rotating stall before its inception, and shows some promise for the early recognition of surge and stall.

The use of artificial intelligence to speed up the detection of these flow instabilities has been shown to have great potential for implementing the monitoring and control process. The utilization of artificial neural networks and correlation matching for the detection process has been demonstrated. Pattern recognition and expert systems are also available techniques for the identification of rotating stall and surge in axial-flow compressors.

ACKNOWLEDGEMENTS

I wish to express my thanks to my major professor Dr. Ching Lo for his help and guidance through the course of this thesis. I would also like to give my thanks to the other members of my committee, Dr. Roy Schultz and Dr. Charles Limbaugh.

I am grateful for the help that Dick Womack and Jim Shelton gave me during my two summers at Arnold Engineering Development Center working on this project.

I wish to thank my family and friends. I thank my parents for their support and encouragement throughout my studies, and I thank Rhonda for her love and understanding during my time at UTSI.

TABLE OF CONTENTS

CHAPTER **PAGE**

TABLE OF CONTENTS

CHAPTER **PAGE**

LIST OF TABLES

LIST OF FIGURES

INTRODUCTION

The axial-flow compressor is a very important piece of machinery in the aerospace world. It is one of the primary components of aircraft turbine engines and compressors provide the wind in wind tunnels. Axial-flow compressors can vary in size from a few feet to tens of feet in diameter. In order to run it as efficiently as possible, and to prevent major damage from occurring, flow instabilities such as rotating stall and surge must be prevented from taking place or dealt with soon after their inception. Surge is defined as the air flow in the axial-flow compressor oscillating back and forth and rotating stall is a region of detached flow rotating around the compressor at a velocity slower than the rotor blades are rotating. Rotating stall occurs when the flow over one blade stalls because of a degradation of the upstream flow.

The compressor is usually operated over a wide range, and depending on the flow conditions, there is a chance that flow instabilities like surge or stall may be experienced over this range.

While operating a compressor with a rotating stall, the flow in the test section might appear to be within normal operating parameters, damage is slowly occurring to the stressed rotor and stator blades. A surge, however, is very noticeable and will change the air flow through the test section, quickly weakening the overstressed rotor and stator blades. If these two phenomena are allowed to continue, major damage to the axial-flow compressor will occur, possibly costing in the millions of dollars and injury to the people in the area.

In wind tunnels, such as those operated at the Arnold Engineering Development Center (AEDC) located at Arnold Air Force Base, Tennessee, the axial-flow compressors are monitored by people called compressor operators. The operators monitor temperatures, pressures, and, in the two large wind tunnels, the stresses experienced by some of the rotor and stator blades in each stage of the compressor. When a surge takes place it is easily detected and corrective procedures are soon taken. A rotating stall, on account of its subtlety, can remain undetected for an extended period of time if the operator is inexperienced or preoccupied with other things and not watching closely. And, when it is detected, operators tend to let it continue for a few minutes in order to ensure that it is a rotating stall and not some temporary fluctuation.

Because of the damage that can occur if corrective actions aren't taken immediately and the fact that the compressor may be operating with a flow instability for a period of time, there is a desire to correct them as early as possible, even before they occur, if possible. A number of methods exist, based on different types of sensors, which can identify the flow instabilities. The types of sensors used include: hot-wire anemometers, thermocouples, pressure transducers, strain gages, optical sensors, and acoustical sensors. Each of these is capable of detecting rotating stall and surge, and each has their advantages and disadvantages.

To utilize these sensors to their greatest potential for detecting and identifying flow instability, and speed up the detection of rotating stall and surge, artificial intelligence (AI) procedures are recommended in this study. AI has the capability of alleviating the compressor operator from continuously watching over the axial-flow compressor performance gages with the great concentration needed to detect these flow instabilities. Some of the forms of artificial intelligence procedures that can be used for performance and health monitoring, and process control are artificial neural networks, pattern recognition, correlation matching, and expert systems.

The purpose of this study is to examine the different sensors that can be used for the detection of rotating stall and surge, examine some of the different methods of artificial intelligence that can be used to monitor the axial-flow compressor, and show that artificial neural networks and correlation matching have the ability to detect a rotating stall.

The study is presented as follows. Chapter 1 is a review of the axial-flow compressor from both a historical and a technical overview. The way compressors behave is explained so that sensor applications can be clearly understood. Chapter 2 is a review of surge and rotating stall phenomena, again provided in order to help clarify how certain sensors detect these damaging flow instabilities. Chapter 3 contains a review of the different types of sensors available for detecting rotating stall and surge in axial-flow compressors. Chapter 4 is a review of the various forms of artificial intelligence that can be employed to monitor the sensors in the compressor for a flow instability. Chapter 5 contains the final conclusions and recommendations for this study. Appendix A contains the strain gage data from a wind tunnel at AEDC operating at Mach 1.2, and the normalized values actually used in the neural network and correlation matching. Appendix B contains the final results from the correlation matching, and a printout of the computer program used.

CHAPTER 1

THE AXIAL-FLOW COMPRESSOR

Historical Development

The basic fundamentals of the operations of a multistage axial-flow compressor, also known as an axial compressor, were first presented to the French Academie des Sciences in 1853 by Tournaire. Sir Charles A. Parsons, in 1884, patented the use of a multistage reaction-type turbine in reverse producing one of the earliest experimental axial compressors (Gostelow, 1984). He later incorporated his primitive axial compressor into blast furnaces. These early models were extremely inefficient because the turbine blades were not designed for increasing pressure in the desired flow direction (Johnsen, 1965), but were adequate for power generation. In 1901 Parsons built and patented an axial-flow compressor but because of inaccurate blade angles the compressor's efficiency was no more than 60%. In patent No. 3060, *Improvements in Compressor and Pumps of the Turbine Type*, he explains:

> "My invention consists in a compressor or pump of the turbine type operating by the motion of sets of movable blades or vanes between sets of fixed blades, the movable blades being more widely

spaced than in my steam turbines, and constructed with curved surfaces on the delivery side, and set at a suitable angle to the axis of rotation. The fixed blades may have a similar configuration and be similarly arranged on the containing casing at any suitable angle (Horlock, 1958)."

Around the beginning of the twentieth century, with the Wright brothers, in 1903, testing airfoils in their home-made wind tunnel, attempts were made to increase the efficiency by designing blades specifically for axial compressors using blade theory. These attempts only produced modest increases in efficiency, increasing them to a little over 50%. This was on account of much of the fundamentals were still unknown.

With the advent of World War I came an increase in research on fluid mechanics, aerodynamics, and compressors. The work of the Wright brothers was expanded into the wind tunnel testing of different biplane arrangements. Using isolated-airfoil theory, an increase in axial-flow compressor performance was realized along with an increase in efficiency. These compressors were found in ventilating fans, air-conditioning units, and steam-generator fans during this time period.

In the 1920's, compressors were used in turbine engines. This improvement in efficiency was the result of the increase in information on the aerodynamics of airfoils and aircraft. Axial-flow compressor blades were being designed by regarding each blade as a separate airfoil. Two-dimensional flow theories were first developed in this period, compressors and turbines of the early 1900's were designed using one-dimensional flow theory (Hawthorne, 1964). Around 1930 came the application of aerodynamic theory to three-dimensional flows in compressors and turbines. With the 1930's came materials that were appropriate for high temperature gas turbines.

Sergei A. Chaplygin, in 1911, first developed the theory of cascades. His first work involved flat plate cascades and was extended to airfoils with camber and thickness in 1933. During 1919, Wood, Bradfield, and Barker perceived that adjacent blades would disrupt the flow and this led to the first cascade experiments. Their discovery that the cascade effect was the reason for the difference between simple airfoil theory and experiment was of major importance. In 1928 came considerable cascade experimentation by Christiani in Germany and by Harris and Fairthorne in England. During the later half of the 1930's, axial-flow compressors designed in England extensively used the data resulting from Harris and Fairthorne. This resulted in an increase in efficiency (Gostelow, 1984).

With the 1930's came the realization of what air superiority meant during war, and this led to a greater interest in axial compressors and eventually to the addition of efficient superchargers to reciprocating engines. Aircraft equipped with these supercharged engines had a greater engine power output and improved high-altitude performance. Turbojets were being looked at for the next step in the desire for an increase in airspeed and altitude. The Royal Aircraft Establishment (R.A.E.) in England started the development of axial-flow compressors for jet propulsion in 1936, climaxing in the F.2 engine in 1941 (Johnsen, 1965). They had developed and tested, by 1938, axial compressors with pressure ratios of 2.5 - 3.0 and efficiencies greater than 80%, and by 1941 a pressure ratio of 3.9 with an efficiency of 85% (Horlock, 1958). Germany and the United States also had their own programs for increasing the performance of axial compressors, and these led to their own advanced engines, including the German Jumo 004 jet engine the first flying jet engine with an axial-flow compressor. The idea of using supersonic compressors took place in Germany in 1935 by Weise, Encke, and Betz who perceived of all of the possible capabilities of using supersonic flows in axial-flow compressors (Hawthorne, 1964). Supersonic compressors were studied in 1941 in the United States by Redding and Kantrowitz but because early tests were discouraging their study was discontinued for the time being.

Among the advances coming out of these programs were a higher pressure ratio per stage through high blade cambers and closer blade spacing. This led to the abandonment of isolated-airfoil theory because of the interaction of the flow pattern among several blades. A cascade aerodynamics theory was developed specifically to handle the problems of the close blade spacing, and along with experiments of airfoils in cascades came the knowledge of how to design axial-flow compressors with these advances.

Since the end of World War II, a substantial investigation has been conducted on increasing the performance of compressors and gas-turbines by expanding their aerodynamic boundaries. An example of this has been the increase of inlet Mach numbers without a sacrifice in efficiency (Lieblein, 1952). Blade loading has also seen much research, with the result that increases in the blade loading can be tolerated today in axial compressors (Lieblein, 1953). Another area that has seen greater research and comprehension is fluid flow through axial compressor blades. Recently, the application of methods such as finite element and finite difference to cascade flows has led to considerable advancement. By the late 1950's, axial-flow compressors were producing pressure ratios of 6.0 - 7.0 and efficiencies of 86% - 90%. Today, it is not uncommon to see axial compressors with pressure ratios of 23 and an efficiency of 90% (Cumpsty, 1989). Some of the reasons for this increase in pressure ratios is the increase in solidity and decrease in aspect ratios of the compressor blades.

In 1945, A.R. Howell published a 10-page paper concerning the design of an axial-flow compressor that was read and accepted widely. The National Advisory Committee for Aeronautics, in 1956, published a guide that was over 1000 pages on the design of an axial compressor (Hawthorne, 1964). From this one can see how much of an increase in the knowledge of axial-flow compressors there was in this eleven year span.

Basic Principles

The basic purpose of an axial-flow compressor is to increase the total pressure of the air flow using shaft work (Johnsen, 1965). Since their inception, there have been continuous improvements like increasing the pressure ratio per stage, increasing the efficiency, and by reducing the weight. A drawing of a compressor located at AEDC, used for the work contained here, can be found in Figure 1.1.

The main parts of the axial compressor are the inlet guide vanes (marked S-1 in the drawing), the rotor blades (marked A, B, and C), the stators between each rotor blade (marked S-2, S-3, S-4), and the outlet guide vanes (marked S-5). The association of a row of rotor blades and a row of stator blades combine to form one stage in the compressor. These are essential because they add energy to the flow.

The inlet guide vanes turn the flow so as to meet the first row of rotor blades at the right incidence angle. Each rotor row adds kinetic energy and increases the static

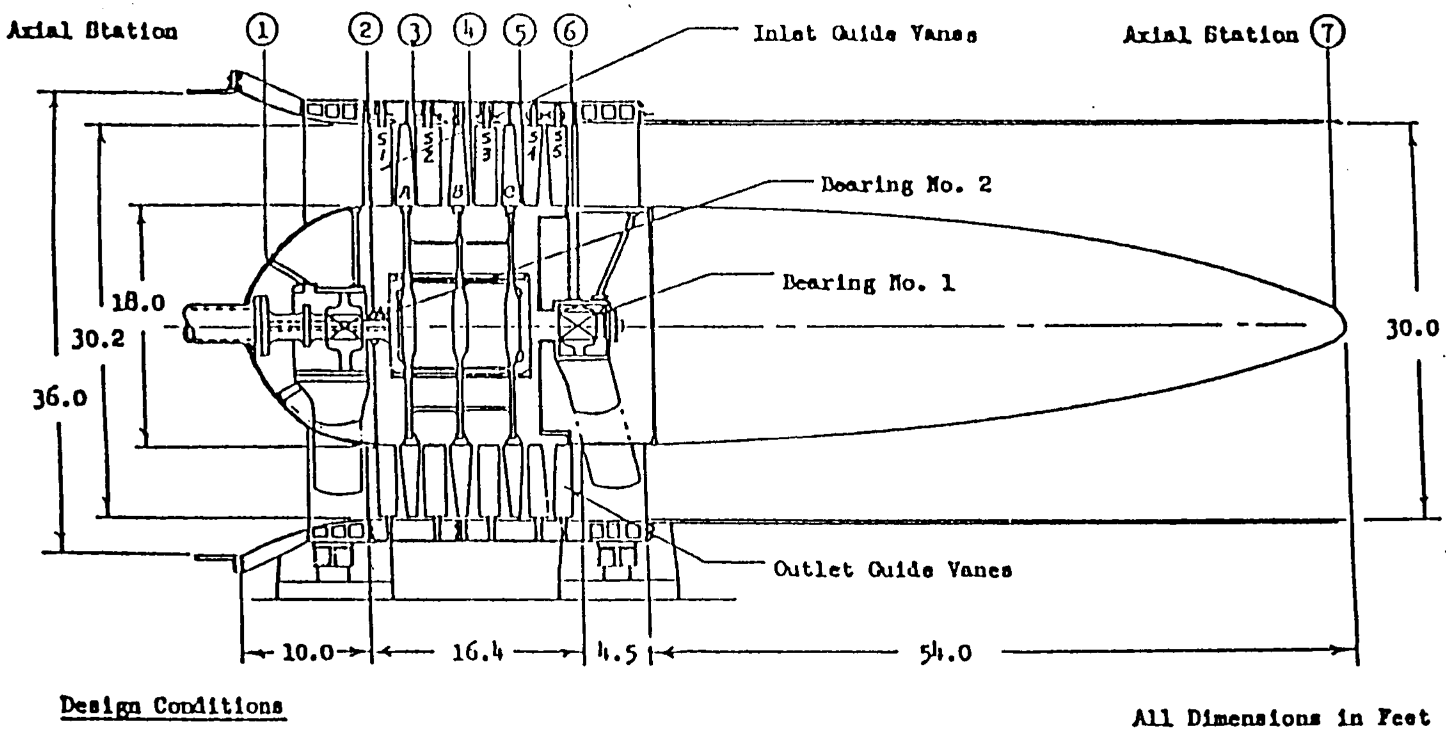

<u>Design Conditions</u>

Tip Speed 942 ft/sec (Absolute)
Hub Speed 565 ft/sec (Absolute)
Design Pressure Ratio 1.385
Design Inlet Volume Flow 200,000 cfs
Flow Coefficient 0.47
Work Coefficient 0.308
Inlet Axial Velocity 442 ft/sec

Figure 1.1 Axial-Flow Compressor, C1 (Lo, February 1991) pressure along with the flow's total temperature and total pressure. The stator rows decrease the kinetic energy by decreasing the rotation of the flow which effectively increases the static pressure. It also provides the correct incidence for the next row of rotor blades. The outlet guide vanes return the angle of the flow to its normal direction. The air flowing through the compressor changes, along with an increase of the total pressure there are variations in pressure, temperature and velocity. The area of the compressor in gas turbine engines decreases as the density of the flow is increased on account of the compression of the air.

The rotor and stator blades have some characteristics in common with the wings of aircraft but they also have many differences. Compressor blades, first of all, rotate in a confined space and have to deal with the effects of the boundary layer on the compressor wall. There is a large variation of the flow along the span of the blade because of this. The rotor and stator blades don't act alone but are surrounded by other blades and rows of blades.

Axial-flow compressors must be planned carefully in order to work efficiently. They are designed with the pressure ratio over the entire unit as one of the primary parameters. The fewer the number of rotor stages there are, the more efficient the compressor. If the material used to make the blade is strong enough only a few rotor stages are needed because each stage is capable of handling a larger pressure ratio. The larger the chord length is in relation to the span, the lower the aspect ratio and higher the hardness of the rotor blade produce a higher pressure ratio per stage (Cumpsty, 1989). Another important factor in the design of an axial-flow compressor is to match the compressor stages so that the flow is smooth. As the flow comes off of a rotor blade it has to hit the following stator blade at just the right incidence, and as it comes off of this it needs to hit the next rotor blade at the correct angle.

The axial-flow compressor, C1, used for this work has three stages and is part of the 16 ft. transonic (16T) wind tunnel located at AEDC. It is designed to operate with a Mach range of 0.6 to 1.6. There are a total of 97 rotor blades, each being 6 ft. long, and 236 stator blades. The inlet volume flow has the capability of being varied from 160,000 ft.^{3}/sec., with a pressure ratio of 1.11, to 250,000 ft.^{3}/sec., with a pressure ratio of 1.60, through adjusting the stator blades. The compressor is 30 ft. in diameter. Strain gages are attached to many of the rotor and stator blades in C1 and are fed through a slip ring assembly to the monitoring system (Joyce, 1975).

CHAPTER 2

ROTATING STALL AND SURGE

Historical Development

Since the introduction of the axial-flow compressor, rotating stall and surge, two types of flow instabilities, have caused compressor designers and operators immense problems. The occurrence of these instabilities was originally considered as one of the normal operating characteristics of axial compressors. One of the earliest written reports of rotating stall was by Chesire in a British report in 1945 on the occurrence of the phenomena on a centrifugal compressor's inducer vanes in the Whittle engine (Gostelow, 1984). The pattern of the flow during a rotating stall was discovered using simple tufts of wool. Binder, in 1946, executed one of the earliest studies of compressor surge (Duke, 1962). He discovered that the ducts linked to the compressor were one of the primary factors causing this surge. Also during this time, Bullock, Wilcox, and Moses were conducting studies of surge in centrifugal compressors for NACA. In 1949, Pearson and Bowmer noticed the hysteresis effect of the oscillating surge.

Shulze, Erwin, and Westphal in a 1950 NACA report wrote of their detection of an axisymmetric flow in an impulse axial compressor with the help of tufts of wool (Johnsen, 1965). The type of flow was identified by Grant a year later as rotating stall, using hot-wire anemometers. Up to this time, all of the research was based on the assumption that the oscillating surge was sinusoidal and associated with Helmholtz resonances (Duke, 1962). In 1953, Huppert and Benser were one of the first to discover that the oscillations were actually nonlinear. Emmons, Pearson, and Grant gave the world the first extensive study of surge and rotating stall in 1955. Using linear flow theory they were able to accurately predict the rotational velocity of the stall cell. Even though rotating stall and surge are nonlinear phenomena, the only way that they could be analyzed were through linear equations of motion and this limited them to analyzing small pieces of the flow.

Much of the research in the early days was concentrated on detecting and controlling rotating stall and surge in the axial compressor of turbojet engines. A study on the methods of detecting stall and surge was made by Delio and Stiglic in 1954 (Duke, 1962). Attempts were made to control compressor surge in 1955 by Chestnut and Mayer, and in 1959 by Munson, Jr.

In 1958, a book was published by Horlock detailing the state of the art about these two types of flow instabilities in axial-flow compressors (Horlock, 1958). Theoretical and experimental work on rotating stall and surge continued, slowly expanding the knowledge of these two phenomena. Fabri in a 1968 NASA report listed an extensive bibliography on the research up until 1968 on rotating stall. Among the other things discovered since then were Day and Cumpsty's finding that stall cells were not stagnant as past theoretical work had assumed (Day, 1978). The entire compression system's characteristics determined whether rotating stall or surge would occur if an instability was introduced to the system (Greitzer, 1976).

In 1972, Takata and Nagano suggested the use of a finite difference method to solve the non-linear flow equations (Gostelow, 1984). Through the use of grooves in the casing of the compressor, the stall margin can be improved, as has been show by Takata and Tsukada in 1977 (Greitzer, 1980).

Stenning, in 1980, derived an equation to predict when a flow instability has the possibility of occurring in an axial-flow compressor. A number of assumptions were made in order to make this prediction. The flow was assumed to be two-dimensional, axisymmetric, incompressible, and that the flow wasn't rotating around the circumference (Stenning, 1980). This, in turn, led to an equation where rotating stall or surge would occur if

$$\frac{\partial(p_2 - p_{01})}{\partial V_x} > 0.$$

The static pressure at the outlet of the compressor is p_2, the average total pressure at the inlet is p_{01}, and the axial velocity is V_x. Experiments, though, have shown that rotating stall has occurred when this value is less than zero (McDougall, 1990).

Fundamentals of Rotating Stall and Surge

During the normal operations of an axial-flow compressor the air flow through the compressor is essentially steady and axisymmetric although rotating. If a flow instability is introduced into the system, through separation of the flow at the inlet, for example, or a change in the speed of the rotors, or other types of flow distortion, the performance of the compressor deteriorates because of the unstable flow. The instability manifests itself as either a rotating stall or a surge. Rotating stall is a region of detached flow rotating around the annulus of the compressor at a rate between twenty and seventy percent of the speed of the rotor (Day, 1978), Figure 2.1. It takes a few seconds to build up and an axial-flow compressor can operate with it for at least a few minutes before it becomes damaging. Surge, as seen in Figure 2.2, consists of the mass flow oscillating back and

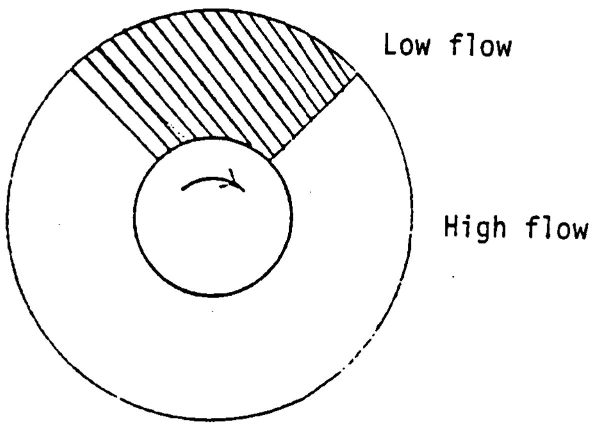

Figure 2.1 Rotating Stall (Andrew, 1985)

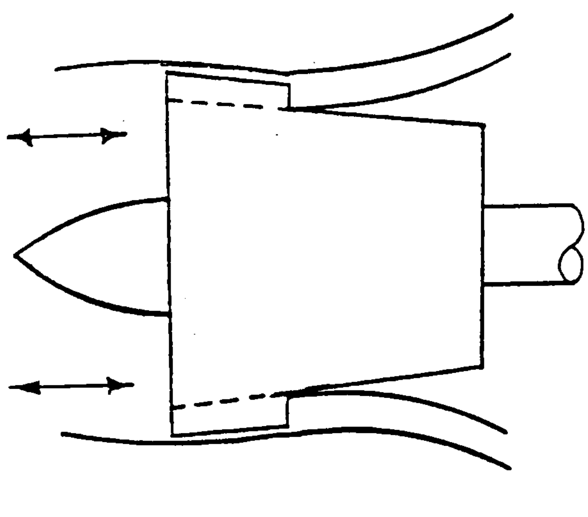

Figure 2.2 Surge (Andrew, 1985)

forth through the compressor. During a surge, the changes in the compressor are severe enough that the compressor can't handle more than a few minutes before it is seriously damaged.

In looking at a map of the performance of an axial compressor, Figure 2.3, a solid line dividing this map can be seen along with lines for different rotational speeds. This line is known as either the surge or the stall line. On the left side of this line surge and rotating stall are known to occur because the flow is unstable. Rotating stall and surge may still occur on the right side of this line if the flow becomes unstable as a consequence of an instability. A second line running parallel to the surge

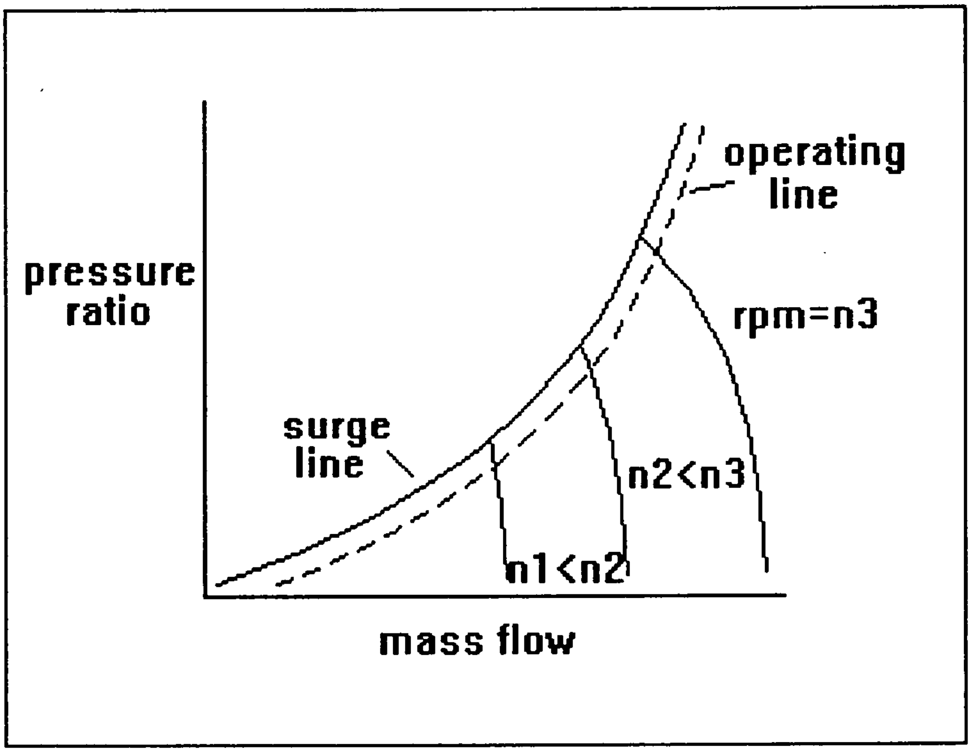

Figure 2.3 Compressor Performance Map

line is known as the operating line. This provides a safety margin for the operation of the compressor, in order to prevent it from experiencing unstable flow. The closer this line is to the surge line the greater the efficiency of the axial compressor, but the greater is the danger of incurring stall or surge.

As stated before, rotating stall consists of flow detaching itself from rotor blades. This flow becomes detached because, as a consequence of some flow instability, the angle-of-attack at which the flow meets the blade increases. This increase in angle-of-attack causes part of the flow to be diverted to the adjacent blades, increasing the angle-of-attack and thereby stalling the next blade and decreasing the flow's angle-of-attack on the previous blade resulting in normal flow over that blade. As this occurs the region of stalled flow, also called stall cell, continues moving from blade to blade thus begetting the name rotating stall. Since the rotor blades are rotating in the opposite direction to the stall cell, the stall region rotates slower than the blades in the same direction. Rotating stall can occur in both incompressible and compressible flow.

There are different types of rotating stall. It may consist of only one stall cell or more than one, based on the mass flow (Greitzer, 1980). The region of stalled flow may only encompass an area near the blade tips, an area near the root of the blade, or the entire blade. This is caused by the variance of the angle-of-attack of the rotor blade. The rotating stall region may encompass just one stage of an axial-flow compressor or any number of stages, depending on the rotor blade's angle-of-attack. The compressor may also pass in and out of rotating stall as the mass flow or rotational speed is varied.

The results of rotating stall can cause serious damage to the axial compressor and its surroundings. The variation of the pressure on the rotor blades can cause them to wear out and eventually break (Duke, 1962). An increase in the internal temperature will result from excessive operation of a compressor experiencing rotating stall, and this will reduce the life of a blade (Greitzer, 1976). The overall mass flow rate and the final output pressure at the exit of the compressor are diminished. Sometimes the reduced performance of an axial-flow compressor operating with a rotating stall is small and cannot be easily detected except by a variation in the noise of the compressor or by some form of high-frequency instrument (Cumpsty, 1989).

In a typical surge, the compressor operates normally until some type of instability disrupts the flow and causes the operating point to exceed the surge line, Figure 2.3. Within milliseconds the flow is axisymmetrically reversed in flow direction (back towards the compressor inlet). During this, the system downstream of the compressor depressurizes causing the flow to reverse its direction again and revert to normal flow direction (towards the compressor outlet). After the system reaches its operating pressure ratio, if the cause of the instability is still present, the axial compressor will experience another surge. This process keeps repeating itself until the instability is removed. During surge the axial-flow compressor "may pass in and out of rotating stall as the mass flow changes with time (Greitzer, 1976)." Rotating stall can also cause surge if located near the rear of the axial compressor.

In high speed compressors the reversal of flow can be carried out with a strong shock wave (Mazzawy, 1980). This shock wave can cause physical damage by deforming the casing or inlet, or by changing the angle of the rotor or stator blades. In low speed compressors the surge manifests itself as a moderate pulsing of the flow. Surge occurs only in flows that are compressible (Stenning, 1980).

During a surge many of the conditions the compressor experiences during rotating stall are present. The exit pressure is reduced, the inlet pressure increases, and there is a general pressure fluctuation inside the compressor. The internal temperature of the compressor increases, especially at the inlet. The rotor blades are stressed by the oscillating flow. The compressor's noise changes.

CHAPTER 3

INSTRUMENTATION FOR THE DETECTION OF FLOW INSTABILITIES

In order to understand the detection of flow instabilities, like rotating stall and surge, one must first review the possible changes in the flow as it proceeds through an axial-flow compressor. In a stall cell there is an appreciable reduction in the mass flow, a fluctuation in pressure, an increase in temperature, an acoustic resonance, and a vibratory stress as the rotor blades pass through the stall cell. A surge is a complete reversal of the mass flow which causes a high blade stress, a decrease in the pressure ratio, a sizeable temperature increase in some compressors, and a variation in the sound of the compressor. The size of these changes can vary greatly depending on the design and size of the compressor, some may not be noticeable at all.

Hot-Wire Anemometers

The hot-wire anemometer is an instrument which can be used for the detection of rotating stall and surge through their mass flow fluctuations. They are currently being used in many studies of rotating stall and surge. The frequency range for common hot-wire anemometers is usually 10 - 20 kHz (Laurence, 1952). They can detect rotating stall or surge within seconds of their onset.

The primary advantage of a hot-wire anemometer is that it can quickly detect mass flow change. This leads to one of the disadvantages, every time a variation in the mass flow occurs it is not necessarily associated with rotating stall or surge. A monitoring system would need to be set up that would be able to distinguish from normal operating changes and a flow instability. If there is a periodicity to the mass flow fluctuations then the chances are strong that some form of rotating stall is present. If a flow reversal is detected by a sudden decrease of the flow over the entire diameter of the compressor then there is probably a surge occurring in the axial-flow compressor. Another disadvantage is that hot-wire anemometers are fragile and expensive. They are not usually used in normal day-to-day operations because of this fact, usually they are used only in studies and experiments where their usage is controlled and somewhat limited. The use of hot-wire anemometers in axial-flow compressors can quickly detect the onset of rotating stall or surge but only after it has fully developed.

Thermocouples

Fast-response thermocouples are used to detect changes in temperature, durable and not very expensive. They are currently used in many axial compressors for the detection of rotating stall and surge. Thermocouples can detect the onset of these flow instabilities within a few seconds. They are mainly used in small compressors, like the Plenum Evacuation System (PES) compressor at AEDC (Daniel, 1979), on account of the relatively constant temperature distribution across the diameter of the compressor during normal operations. For them to detect temperature variations in large compressors there would have to be a number of extremely sensitive thermocouples located around the circumference of the compressor, though this set up would not be able to detect a rotating stall cell located at the root of the rotor blade.

If a periodicity is detected in the temperature change then the chances are good that a rotating stall is present, if there is a rapid unexplainable increase in the temperature then the possibility of a surge being present is strong. Thermocouples are effective but they can only indicate that the rotating stall or surge is present, it cannot be used to predict the occurrence of these phenomena in the compressor.

Pressure Transducers

Pressure transducers are very effective at detecting rotating stall and surge, within seconds of their beginning. They are able to detect the periodicity of the pressure fluctuations as the stall cell rotates around the axial compressor, and also the changing pressure ratio as the compressor surges. A new discovery is that high response static pressure transducers located on the casing wall around the circumference of the compressor are effective in detecting the inception of rotating stall (Garnier, 1991; Inoue, 1991). Since rotating stall can occur before surge, this method could lead to the early detection of surge.

A precursor to rotating stall was first detected by McDougall, Cumpsty, and Hynes (1990). They discovered "small disturbances rotating about the machine just prior to the onset of stall" (Garnier, 1991). These prestall waves moved around the circumference of the axial-flow compressor at approximately the same speed as the rotating stall frequency. They consist of a region near the wall of the compressor where the pressure fluctuates greatly. The amplitudes of these waves are usually less than 5 percent of the amplitude of the stall. It starts anywhere between 10 - 200 rotor revolutions before rotating stall starts and can grow into a full-fledged rotating stall. If during this time the cause of these waves can be found and corrected then the rotating stall can be averted. It can be detected easiest at the stages in which the stall is developing. If the flow is being affected by a distortion at the inlet then the initial detection of the prestall waves is harder to detect.

The ability of the compressor system to damp out the causes of prestall waves can be linked to how easily the axial compressor will develop a full rotating stall. If the driving force behind the flow instability is stronger than the damping force of the compressor the prestall waves will start developing and eventually turn into a rotating stall and possibly a surge.

The major disadvantage of this method is that it is still in the early stages of research. The researchers believe that prestall waves can be found in each compressor but they don't understand enough about the phenomena to be completely confident (Garnier, 1991). Indications are that the strength and duration of the prestall waves will vary depending on the axial compressor construction and in some compressors they might be difficult to detect.

Strain Gages

Strain gages are the most prevalent sensor for the detection of rotating stall and surge. They measure the stress in the compressor's rotor blades and stator blades and can catch the change in blade stress associated with these phenomena within seconds after they start. As stated previously, the blades experience an increased stress during a rotating stall and surge. At least one blade per stage should have a strain gage attached. A surge is very easy to detect because the fluctuation of the stress caused by flow reversal is very large and distinctive. The rotating stall, however, is more subtle. There may only be a slight increase in the stress level as the blades pass in and out of the rotating stall cell, but this will also shorten the fatigue life of the blades. The axial compressor would have to operate for a period of time with this subtle increase in stress level for damage to occur. Strain gages also pick up normal operating changes which sometimes can appear as a rotating stall. The strain gages can be connected to a frequency spectrum analyzer which exhibits the spectrum data (Province, 1979). If watched closely enough the onset of rotating stall can many times be detected, but with multistage compressors watching all of the strain gages can be difficult.

The advantage of using strain gages is that a surge is easily detected and corrective procedures can be enacted immediately. A rotating stall can be detected by an experienced operator within a few minutes and rectified soon after.

One of the disadvantages is that these phenomena can't be detected and corrected until they are fully developed and causing damage. An axial-flow compressor at AEDC was operating with a rotating stall for 30 minutes, once, and there was no apparent damage (Womack, 1991). Another time a compressor was operating, unknowingly, with a rotating stall for three hours and there was extensive damage. Another disadvantage is that connecting this rotating system to the monitors outside of the axial compressor can be quite difficult. The strain gage can also be hard to attach to the blades and it has a high rate of failure (Nieberding, 1977).

Optical Sensors

The optical sensor consists of a light source attached to the outer wall of the compressor being focused on the trailing edge of rotor blades as they pass this light source and the reflection of this light being picked up by fiber optics. Using this method the torsional and bending stress of the blade can be found (Fowler, 1979). The final results are similar to those of strain gages. The stress in the rotor blades would increase during rotating stall and surge, and with optical sensors located at each compressor stage, be detected as easily as it would be if strain gages were used, a few seconds after it starts.

Besides the reflection off of the trailing edge blade, three other pieces of information are needed to calculate the stresses. A reflection off of the midchord of the blade, along with a sensor that indicates the passage of each blade pass the optical sensor and another sensor that records each revolution of the rotor stage. The difference in the time between the trailing edge reflection, the blade sensor, and the revolution sensor with the midchord sensor is proportional to the stress in the blade (Fowler, 1979).

This system has a few advantages over strain gages and might be a good replacement. Every single rotor blade could be monitored as it passes the sensor and the detection would only be limited by the time it takes for the rotating stall cell to rotate pass the sensor. Strain gages are difficult to attach to the rotor blades, whereas the optical sensors can be attached to the compressor's outer wall or in a window in the outer wall. When a strain gage fails the entire rotor blade has to be taken out, the optical sensor, though, can be easily changed. There is also a chance that the strain gage may affect the aerodynamics of the rotor blade, the optical sensor using a window wouldn't affect the performance of the blades. Connecting the optical sensors to a monitoring system would be much easier that connecting strain gages that are mounted on rotor blades that are being rotated around the compressor at a high speed.

The disadvantage of this system is the same as that for the strain gages, rotating stall and surge can't be detected until they are completely developed. Also, if mounted in windows on the casing wall, the windows may eventually become dirty which would affect the optical sensors.

Acoustical Sensors

As rotor blades rotate in an axial-flow compressor they vibrate which produces a sound. As the pressure in the compressor changes so does the vibration and the resulting sound (Parker, 1984). An acoustical sensor would be able to monitor the sound and detect any changes within a few seconds. The onset of rotating stall and surge would change the pressure thus changing the acoustical resonance of the compressor.

The advantage of this method is that it just requires the placement of a few acoustical sensors and that, depending on how much the sound changes, the sensors might be placed externally around the compressor. They would be able to monitor the entire axial compressor and would be easy to replace if they fail.

The major disadvantage is that not enough experimental work has been conducted on the acoustics of axial-flow compressors. Some compressors may not have a measurable change in its sounds as the pressure changes, this would be a result of the compressor's design. This method will probably not be able to detect rotating stall and surge until they are fully developed. There is a chance it may be able to pick up the small pressure changes associated with prestall waves but that will have to be left to further research.

The raw signals from each of the previous systems would need to be sent to a monitoring system which would change them to parameters which could be better understood. This would take a few seconds. Up to this point approximately 10 seconds will have passed.

CHAPTER 4

APPLICATION OF ARTIFICIAL INTELLIGENCE

Artificial Intelligence

Artificial intelligence (AI) is a method used to provide a computer with a form of reason and allow it, in a sense, to think. It is a technique in which the human thought process is broken down and written into a computer algorithm. This algorithm has the ability to absorb information, learning something like a person would, without going back and rewriting the algorithm. This provides a flexibility that a normal computer program would not be capable of, without rewriting the program.

Trying to understand how a person thinks is still a somewhat new and complicated task. We are only beginning to comprehend the thought process, but the basics are understood, people are driven by goals. These goals can be achieved by relating the facts of the situation to a set of rules. One way to characterize intelligence would then be partly based on how complex these facts, rules, and goals can be. A monkey who has the goal of satisfying its hunger by eating a banana, which is located up in a tree, can use his intelligence to reason that he will have to climb up the tree in order to reach the banana or find some way to knock it down. If that banana was located on the moon, he would not have the intelligence to reach it. If a human was hungry and wanted the banana which was on the moon, he could use his intelligence to reason that he alone could not reach it but a rocket could be built with the help of others to take him to the moon and the banana. A computer that used artificial intelligence software that was written with rules for a task like this, given the same goal of getting the banana, using the facts of where the moon is located and with the knowledge of what it takes to get there, should arrive at the same conclusion as the human.

Incorporating artificial intelligence into an on-line monitoring system would allow for the detection of events like rotating stall and surge. With it the detection of these unsteady phenomena will be swifter than it would be with humans and alleviate the compressor operators from closely monitoring machinery like axial compressors.

Artificial Neural Networks

The artificial neural network is a biological model of the human brain and nervous system imitated by a computer. It can be used for "classifying data, modeling and forecasting, and signal processing" (Klimasauskas, 1991). Neural networks have several advantages:

1.) given some sample data, neural networks have the capacity of learning how to carry out a job on their own;

2.) they can adapt themselves according to the training data;

3.) furnished a little bad data, the network still has the capability, even though degraded, to continue operating;

4.) neural networks can operate in real-time;

5.) they can easily be used with today's technology (Maren, 1990);

6.) they have the ability to operate with input data that has noise (Lo, February 1991).

They have one major disadvantage, the inability to interpret data for conditions which they haven't been taught, i.e. new faults. This is a current research topic to identify the new faults. Also, they aren't guaranteed the ability to map every single thing, and with large neural networks there are sometimes long training periods (Wasserman, 1989).

A computer neural network is compromised of artificial neurons, capable of having a quantity of input values, but only one output value, linked to each other by axons. As a neuron becomes energized by its inputs, it discharges, transmitting energy to nearby neurons. As other neurons collect enough power they will in turn discharge, dispersing the energy to other neurons (Artificial Intelligence Tutor, 1991). Organized in layers, these neurons form a neural network.

Through internal feedback, a self correcting method, it is capable of learning and improving itself through its interaction with its environment. Essentially, the function of the artificial neural network is pattern processing (Caudill, 1990). Things are remembered through the links, connecting the neurons, by varying the weights attached to them. It is not influenced by human "experts" but learns everything on its own from what it is taught. Neural networks have been used in a number of manners. They have been used on Wall Street to predict the stock market and buy or sell based on its output. They have mastered speech practically without aid from humans, recognized diseases, composed music, monitored engines, and have many more such accomplishments. They are also being used by the Defense Department for a variety of tasks, including an attempt to develop an airplane that can adjust to its surroundings and be capable of repairing itself (Artificial Intelligence Tutor, 1991).

For this project a neural network was designed using the computer program NeuralWorks Explorer (1988) and strain gage data from compressor rotor blades with the wind tunnel operating at Mach 1.2. The network incorporated sixteen inputs, seven nodes in the hidden layer, and four outputs (Figure 4.1), and used a self correcting method entitled backward propagation in its learning process. In training a neural network, example inputs are entered along with their desired outputs. As the network is fed the inputs and comes up with its own output, a comparison is made to the desired output. The difference is the error and is used to adjust the weights. The process is repeated until all of the sample data sets have been iterated over the desired amount of time. Large data sets are usually iterated over more times than small data sets. Multi-layer networks are excellent in modelling a nonlinear equation (Meyer, 1991).

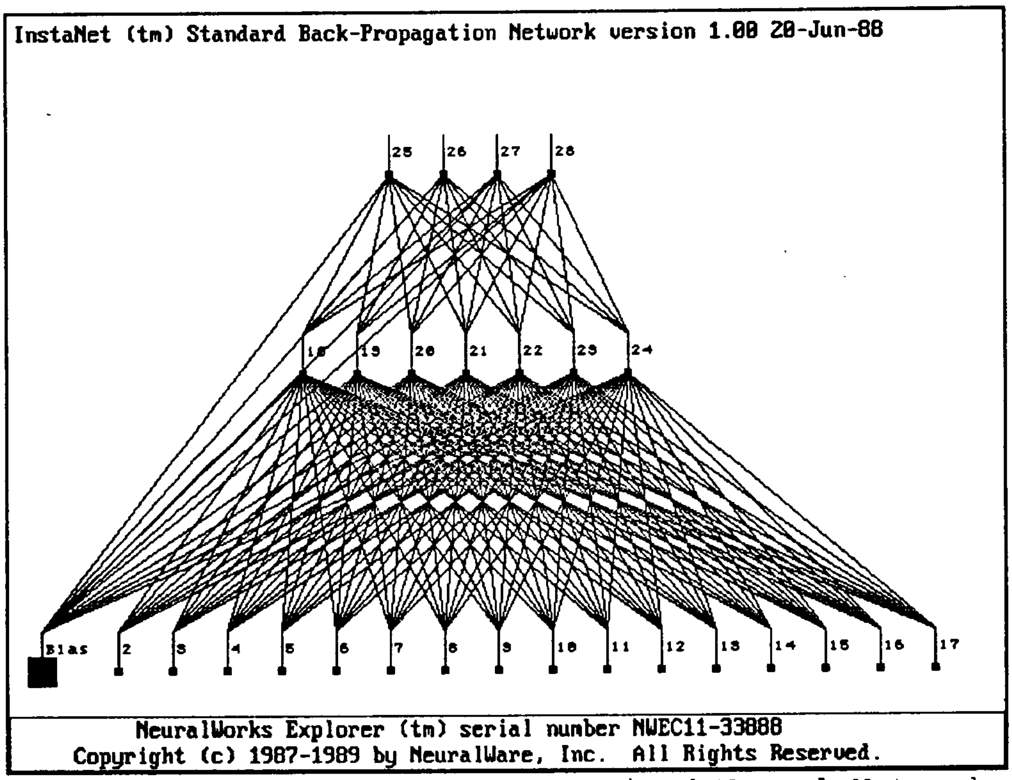

Figure 4.1 Example of an Untrained Neural Network

The test data used in this project was taken at the Arnold Engineering Development Center (AEDC), located on the grounds of Arnold Air Force Base, Tennessee. AEDC houses a large number of wind tunnels among its multitude of testing facilities. Among these wind tunnels is the 16 ft. transonic tunnel in which the data was recorded.

The current method used to detect rotating stall and surge are through the use of strain gages attached to a number of the rotor and stator blades in each row of the axial compressor, and their continuous monitoring by people in the compressor control room. The stress data was recorded on magnetic tape during some tests at Mach 1.2. Utilizing a Spectrum Analyzer the frequency spectrum was then obtained from the data, and "snapshots" of the spectrum were taken by a personal computer and stored on a disk as ASCII files. An example of one of these "snapshots" for normal operations can be found in Figure 4.2. The amplitude of the data can be related to Volts which can then be related to pounds per square inch (psi). What is important here, though, is how the amplitudes compare to each other on the frequency spectrum. Peaks can be found at 10 Hz, which is the rotational speed of the compressor, and at the harmonics of 10 Hz. The rotor blade's natural frequency of 27.5 Hz is the reason that the amplitude at 30 Hz stands out and the blade's second natural frequency of 74 Hz is the reason that the amplitude at 70 Hz is so large.

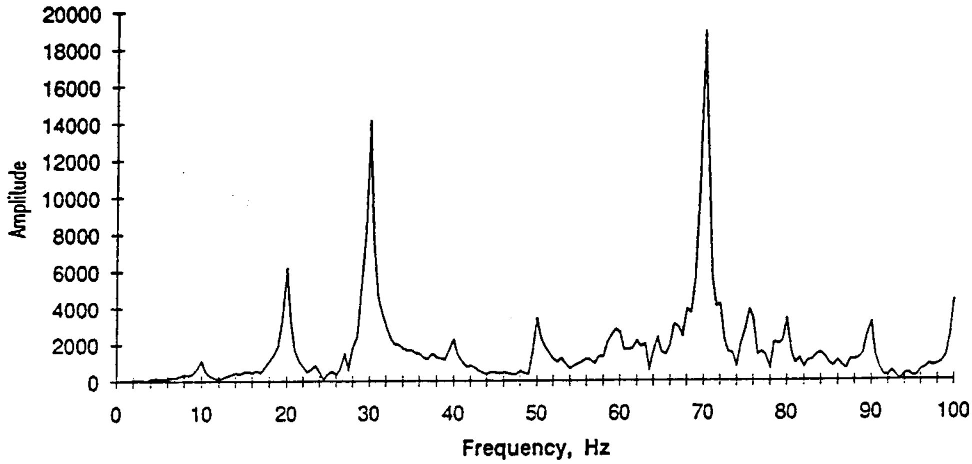

Figure 4.2 "Snapshot" of the Frequency Spectrum for Rotor Blade B01 During Normal Operations

In order to train a neural network, stress data from normal compressor operations and during a rotating stall was needed. The stress data from normal operations was readily available but there was no time in the scheduled operations of the 16 ft. transonic wind tunnel for operating with a rotating stall and it wasn't safe for the compressor to operate under those conditions. With the help of Richard Womack, an engineer with the Calspan Corporation working at AEDC who has had many years of experience with the axial compressor in the 16 ft. transonic tunnel, a sketch of how a rotating stall would appear when compared with normal operations was made. Figure 4.3 shows what the frequency spectrum for rotating stall would roughly look like. In

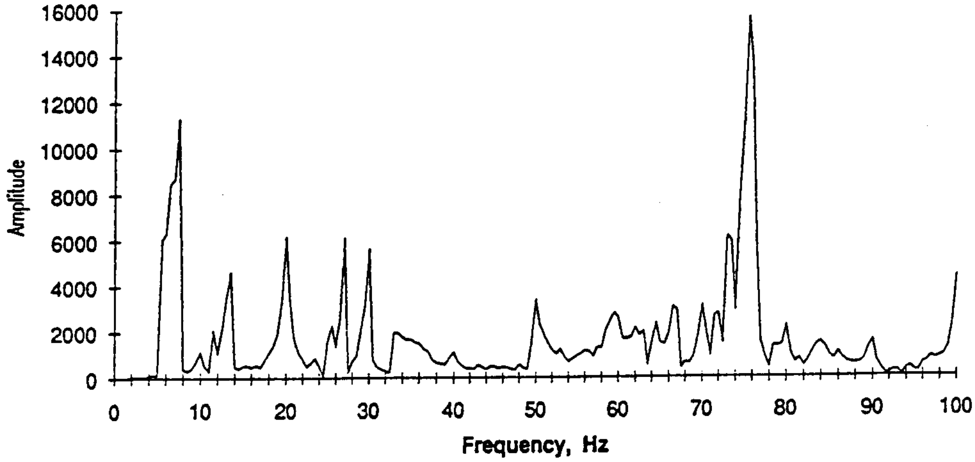

Figure 4.3 "Snapshot" of the Frequency Spectrum for Rotor Blade B01 During a Rotating Stall

comparing the frequency spectrum for normal operations and rotating stall, as shown in Figure 4.4, the difference can easily be seen: the amplitudes at 6.5 Hz and 12.5 Hz are larger than the amplitude at 40 Hz, the amplitude at the blade's natural frequency of 27.5 Hz is bigger than that at 30 Hz, and the amplitude at the blade's second natural frequency of 74.0 Hz is greater than the amplitude at 70 Hz.

The input to the neural network was the amplitudes of the major frequencies, found in Table 4.1. These sixteen inputs were connected to each of the seven nodes forming the hidden middle layer, which in turn were connected to each of the four output nodes, as seen in Figure 4.1. The initial desire was for the neural network to show that it can

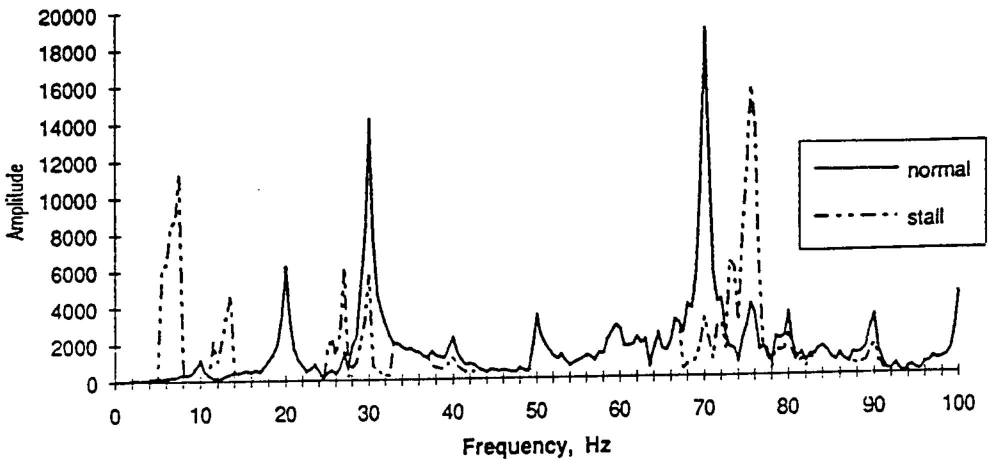

Figure 4.4 Comparison of the Frequency Spectrums for Normal and Rotating Stall Operations of Blade B01

differentiate between the different compressor blades and detect rotating stall. Later on a second case was added, differentiating between the different compressor blades and locating which blade was experiencing the rotating stall.

Each grouping of sixteen amplitudes, from the frequency spectrum at one point in time, will be defined as a data set. Usually when a network is trained there is a desire for a large number of data sets. The data for Mach 1.2 was limited to only three data sets from a couple blades in each of the three stages of the axial-flow compressor of the transonic tunnel. The input file to the artificial neural network utilized three data sets for blades A13, B01, and C16. This data along with their associated synthesized

Table 4.1 Frequencies

Frequency	Comments
6.5 Hz	stall zone frequency
10.0 Hz	rotational speed
12.5 Hz	harmonic of stall zone frequency
15.0 Hz	
20.0 Hz	second harmonic of rotational speed
25.0 Hz	
27.5 Hz	blade natural frequency
30.0 Hz	third harmonic of rotational speed
35.0 Hz	
40.0 Hz	fourth harmonic of rotational speed
45.0 Hz	
50.0 Hz	fifth harmonic of rotational speed
70.0 Hz	seventh harmonic of rotational speed
74.0 Hz	blade second natural frequency
80.0 Hz	eighth harmonic of rotational speed
90.0 Hz	ninth harmonic of rotational speed

rotating stall data made up eighteen data sets, found in Table A.1, in Appendix A. Before this can be used by the neural network the data needs to be normalized on a scale of 0 to 1, Table A.2, Appendix A. One final thing needed to be added to this input and that was the desired output. The first output node of the neural network represented blade A13, the second output blade B01, the third output blade C16, and the fourth output showed whether or not rotating stall was being experienced. A number one was used in the output node to indicate what each data set was, whether it was blade A13, B01, C16, and/or rotating stall, and a zero in the output nodes for what it wasn't. Table 4.2 shows what the desired output for the first case looks like and Table 4.3 shows the desired output for the second case.

Once the input training set along with the desired output was established the neural network was trained. In order to find the needed weights, so as to acquire as near as possible the desired output from the know input, the network iterates over the training set. Experience has shown that it usually takes at least a few thousand iterations in order to get the error, the difference between the desired output and the actual output, down to a minimum. This network used a total of 5000 iterations in its training, which just took a few minutes.

Now that a trained neural network was established for the detection of rotating stall the network needed to be tested. Normally non-input data is used for testing but since the data for Mach 1.2 was limited and all of it was used in the training one can only reuse it to test the network and check how closely the actual output is to the desired output. The results of the test can be found in Table 4.4. These results should be compared with Table 4.2 to find how close the actual output is to the desired output. As shown, the neural network worked very well, with the actual output very close to the desired output. Blade A13 should have an output close to 1, 0, 0, 0 and it's

Table 4.2 Desired Output for Case 1

	Do_1	Do_2	Do_3	Do_4
A13-01	1.0000	0.0000	0.0000	0.0000
A13-02	1.0000	0.0000	0.0000	0.0000
A13-03	1.0000	0.0000	0.0000	0.0000
B01-01	0.0000	1.0000	0.0000	0.0000
B01-02	0.0000	1.0000	0.0000	0.0000
B01-03	0.0000	1.0000	0.0000	0.0000
C16-01	0.0000	0.0000	1.0000	0.0000
C16-02	0.0000	0.0000	1.0000	0.0000
C16-03	0.0000	0.0000	1.0000	0.0000
A13-S1	0.0000	0.0000	0.0000	1.0000
A13-S2	0.0000	0.0000	0.0000	1.0000
A13-S3	0.0000	0.0000	0.0000	1.0000
B01-S1	0.0000	0.0000	0.0000	1.0000
B01-S2	0.0000	0.0000	0.0000	1.0000
B01-S3	0.0000	0.0000	0.0000	1.0000
C16-S1	0.0000	0.0000	0.0000	1.0000
C16-S2	0.0000	0.0000	0.0000	1.0000
C16-S3	0.0000	0.0000	0.0000	1.0000

Table 4.3 Desired Output for Case 2

	Do_1	Do_2	Do_3	Do_4
A13-01	1.0000	0.0000	0.0000	0.0000
A13-02	1.0000	0.0000	0.0000	0.0000
A13-03	1.0000	0.0000	0.0000	0.0000
B01-01	0.0000	1.0000	0.0000	0.0000
B01-02	0.0000	1.0000	0.0000	0.0000
B01-03	0.0000	1.0000	0.0000	0.0000
C16-01	0.0000	0.0000	1.0000	0.0000
C16-02	0.0000	0.0000	1.0000	0.0000
C16-03	0.0000	0.0000	1.0000	0.0000
A13-S1	1.0000	0.0000	0.0000	1.0000
A13-S2	1.0000	0.0000	0.0000	1.0000
A13-S3	1.0000	0.0000	0.0000	1.0000
B01-S1	0.0000	1.0000	0.0000	1.0000
B01-S2	0.0000	1.0000	0.0000	1.0000
B01-S3	0.0000	1.0000	0.0000	1.0000
C16-S1	0.0000	0.0000	1.0000	1.0000
C16-S2	0.0000	0.0000	1.0000	1.0000
C16-S3	0.0000	0.0000	1.0000	1.0000

Table 4.4 Actual Output for Case 1

	Do_1	Do_2	Do_3	Do_4
A13-01	0.9806	0.0232	0.0183	0.0082
A13-02	0.9751	0.0136	0.0228	0.0108
A13-03	0.9764	0.0088	0.0203	0.0148
B01-01	0.0003	0.9854	0.0110	0.0133
B01-02	0.0098	0.9841	0.0023	0.0089
B01-03	0.0151	0.9822	0.0025	0.0077
C16-01	0.0048	0.0139	0.9793	0.0037
C16-02	0.0189	0.0058	0.9858	0.0029
C16-03	0.0139	0.0035	0.9831	0.0048
A13-S1	0.0063	0.0001	0.0001	0.9973
A13-S2	0.0076	0.0000	0.0001	0.9975
A13-S3	0.0047	0.0000	0.0001	0.9981
B01-S1	0.0000	0.0109	0.0001	0.9924
B01-S2	0.0002	0.0113	0.0000	0.9864
B01-S3	0.0003	0.0018	0.0000	0.9959
C16-S1	0.0002	0.0000	0.0009	0.9968
C16-S2	0.0005	0.0000	0.0052	0.9904
C16-S3	0.0002	0.0000	0.0032	0.9968

close to that. Blade B01's output is similar to its desired output of 0, 1, 0, 0. The output of blade C16 is close to its preferred output of 0, 0, 1, 0. The output for a rotating stall should be 0, 0, 0, 1, and it is very close to that. Figure 4.5a exhibits the neural network as it might appear if the input data came from blade A13 during normal operations, the larger the node the closer the value is to one, and the smaller it is the closer it is to zero. Figure 4.5b shows the network for blade B01 operating normally, Figure 4.5c shows the normal operations of blade C16, and Figure 4.5d shows the detection of a rotating stall on one of the blades. The purpose of the node labelled "Bias" is to have the capability of adding noise to the entire system, it is therefore connected to every node in the network. If a neural network is trained with some noise it would be able to handle noisy data better. The nodes labelled 2 - 17 are the input nodes, nodes 18 - 24 are the hidden layer nodes, and nodes 25 - 28 are the output nodes. Each of the input nodes are connected to each of the hidden layer nodes which are connected to each of the output nodes.

The numbers that were supposed to be one are within three percent of one which is close enough to be effective and the rest of the numbers are close to zero. This shows that a neural network can differentiate between different compressor blades and detect a rotating stall. The results for the second case, found in Table 4.5 and when compared to

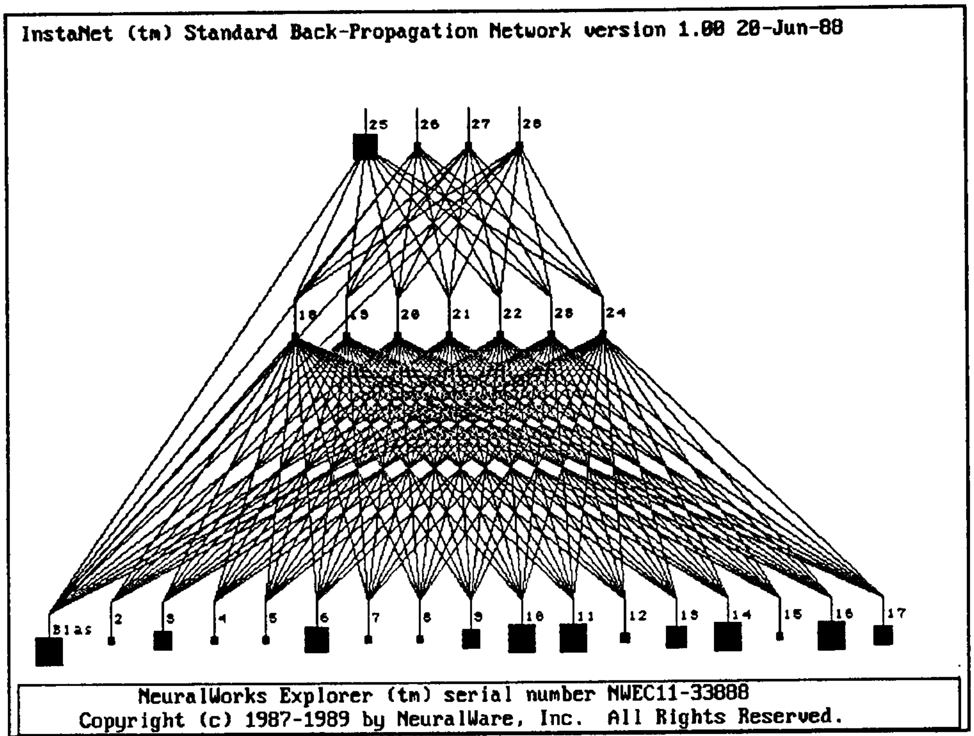

(a) Normal Operations for Blade A13

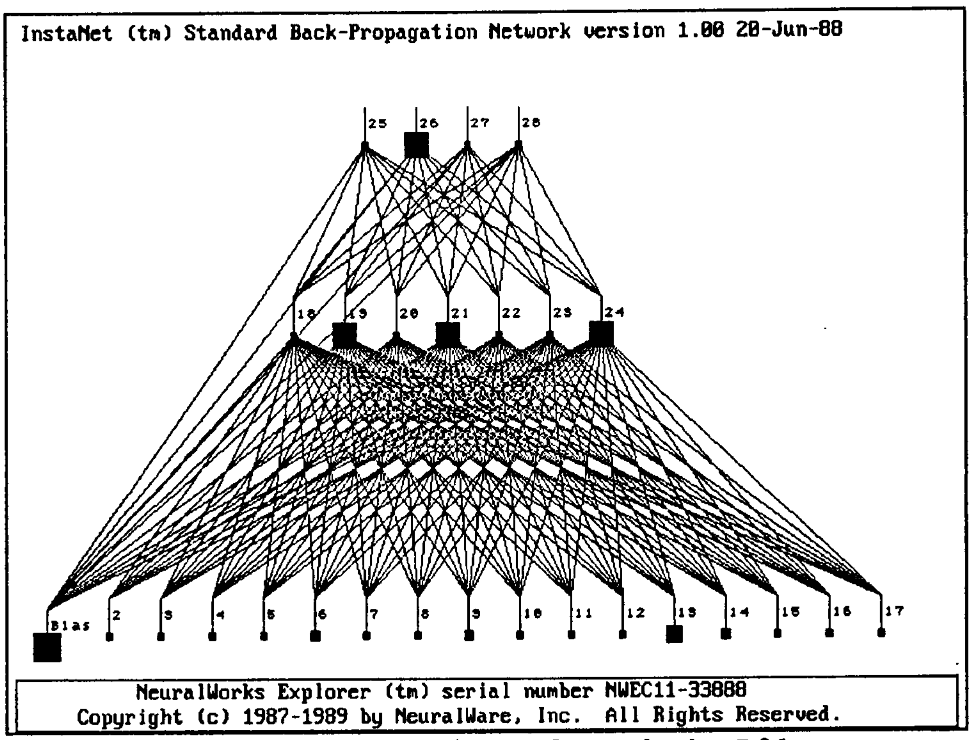

(b) Normal Operations for Blade B01

Figure 4.5 Neural Network for Case 1

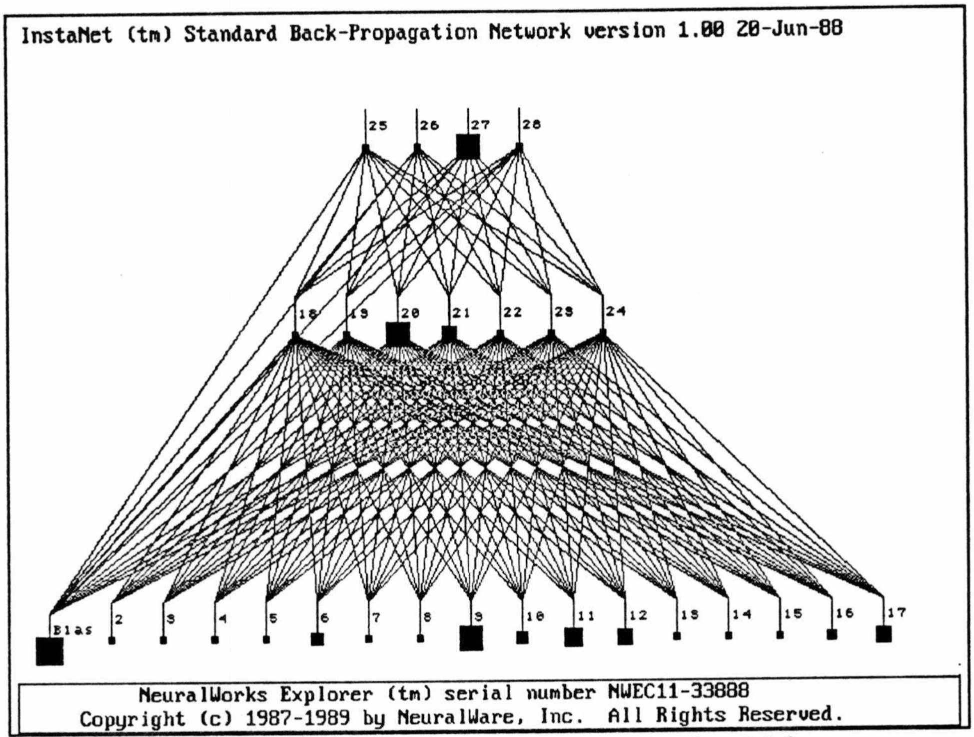

(c) Normal Operations for Blade C16

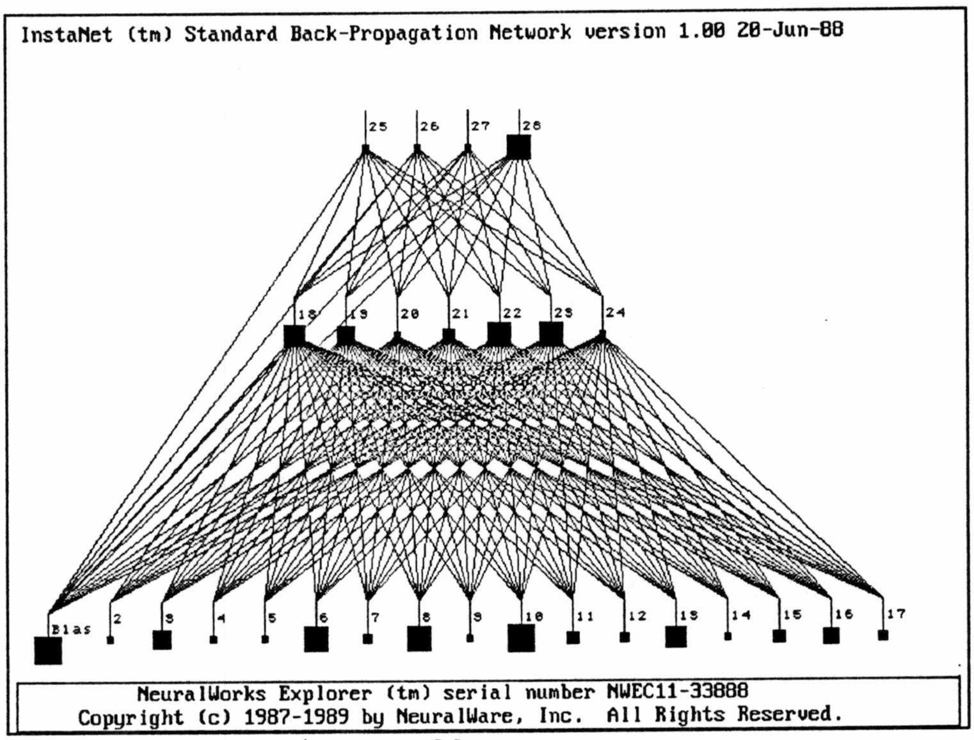

(d) Rotating Stall

Figure 4.5 (continued)

Table 4.5 Actual Output for Case 2

	Do_1	Do_2	Do_3	Do_4
A13-01	0.9843	0.0155	0.0068	0.0128
A13-02	0.9832	0.0082	0.0156	0.0133
A13-03	0.9859	0.0056	0.0213	0.0175
B01-01	0.0000	0.9964	0.0131	0.0147
B01-02	0.0039	0.9923	0.0005	0.0059
B01-03	0.0101	0.9859	0.0004	0.0063
C16-01	0.0028	0.0091	0.9887	0.0060
C16-02	0.0080	0.0035	0.9913	0.0042
C16-03	0.0098	0.0036	0.9890	0.0053
A13-S1	0.9880	0.0110	0.0061	0.9940
A13-S2	0.9867	0.0070	0.0119	0.9944
A13-S3	0.9895	0.0068	0.0096	0.9955
B01-S1	0.0002	0.9966	0.0032	0.9925
B01-S2	0.0060	0.9945	0.0002	0.9848
B01-S3	0.0110	0.9913	0.0002	0.9934
C16-S1	0.0079	0.0036	0.9896	0.9914
C16-S2	0.0099	0.0040	0.9860	0.9876
C16-S3	0.0094	0.0023	0.9930	0.9924

the desired output in Table 4.3, also shows that the network can differentiate between rotating stalls on different blades. Figure 4.6a displays a neural network that has detected a rotating stall on blade A13, Figure 4.6b a rotating stall on blade B01, and Figure 4.6c a rotating stall on blade C16. If blade A13 was experiencing a rotating stall then its output should be 1, 0, 0, 1, and according to Table 4.5 it is very close to that. A rotating stall on blade B01 would be detected by a neural network if its output was near 0, 1, 0, 1, which is close to its actual output. Blade C16 would be encountering a rotating stall if its output was close to 0, 0, 1, 1, which it is.

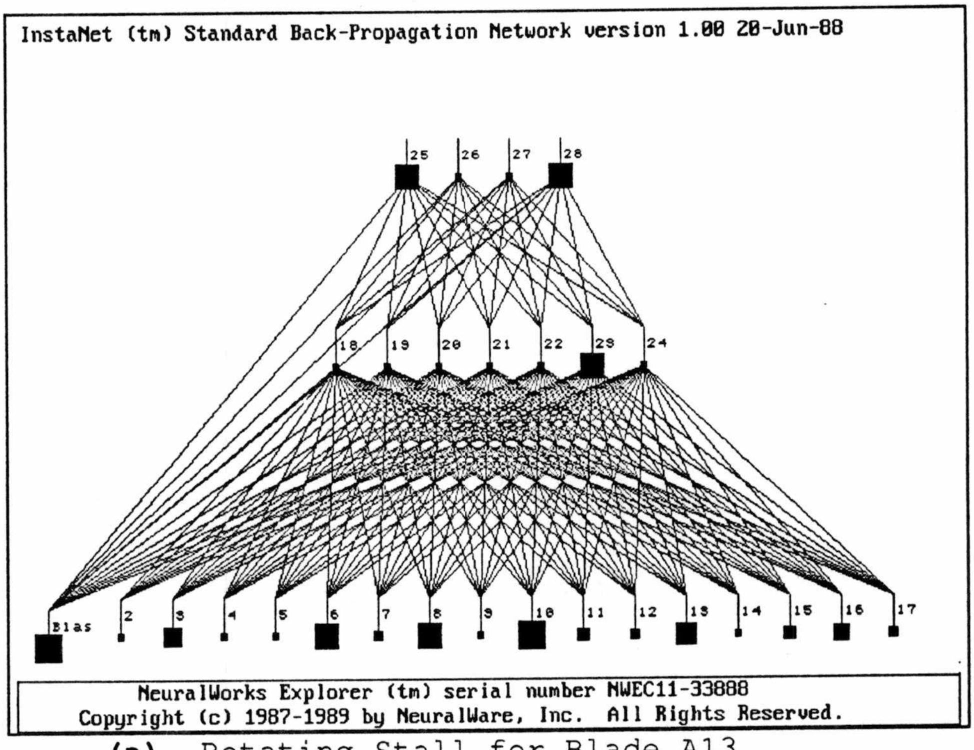

(a) Rotating Stall for Blade A13

Figure 4.6 Neural Network for Case 2

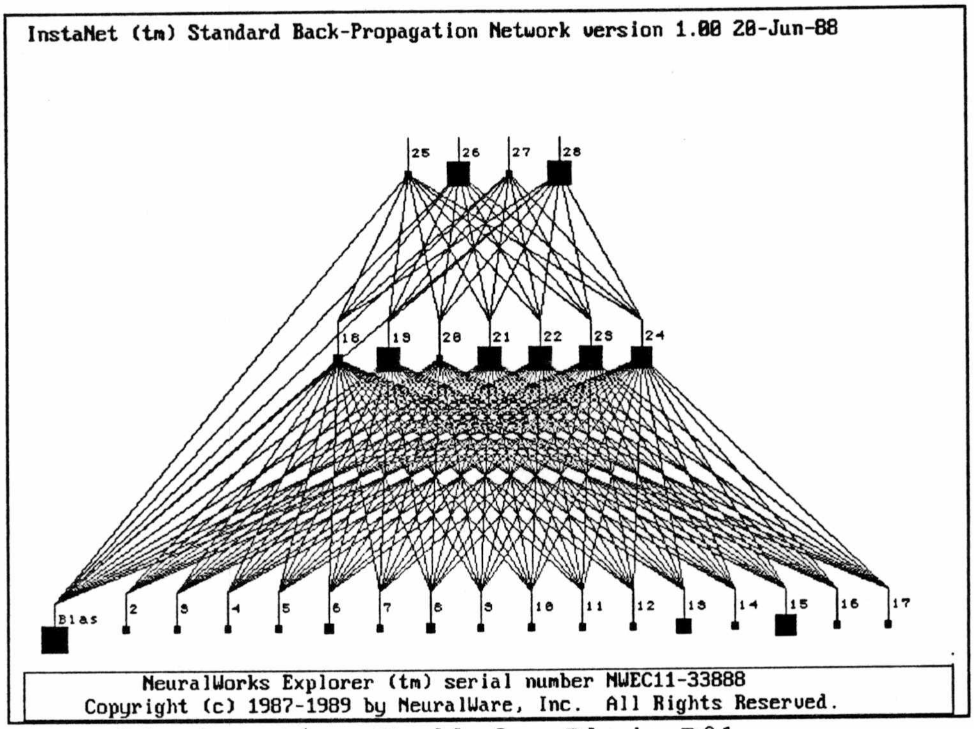

(b) Rotating Stall for Blade B01

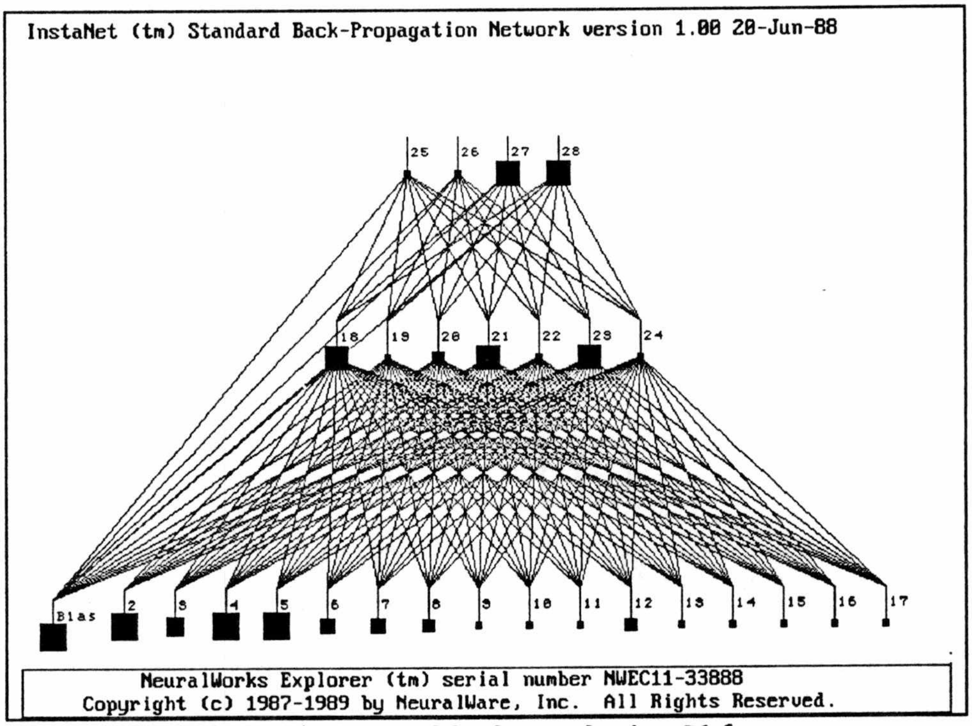

(c) Rotating Stall for Blade C16

Figure 4.6 (continued)

The overall results show that a neural network can be used to monitor and detect rotating stall in an axial-flow compressor for Mach 1.2.

Pattern Recognition - Nearest Neighbor Method

The function of a pattern recognition system is to identify and classify data as to what class, or group, they belong to. This is based on the known features of each class and the features identified from the data. There are two main types of recognition, that of concrete items and that of abstract items (Tou, 1974). Concrete items, like a rose, a song, or a picture, are recognized using something like a persons senses. An abstract item, like recalling an old car or remembering a place visited in the past, doesn't use these senses. The type of pattern recognition that will be covered here is that of the first kind. Examples of pattern recognition being used today are: character recognition, speech recognition, speaker recognition, weather prediction, medical diagnosis, and stock market prediction.

In recognizing something, human beings pick out the distinctive features of that item and try to match it with their past observations. Computers can use a similar method. Once the different features were picked out they could then be compared with the various features of the classes which the computer has previously been trained on. The quality of the pattern recognition system will depend on how closely the training data resemble the actual data that will be used on the system.

A number of basic problems exist when putting together a system which can distinguish between different patterns. The first problem is in the presentation of the data. One way to present this is as a point in n-dimensional space, n being the number of distinctive features, and identified as the point. Below, **x** is the point, shown as

$$\boldsymbol{x} = \begin{pmatrix} x_1 \\ x_2 \\ \cdot \\ \cdot \\ \cdot \\ x_n \end{pmatrix}$$

where each x_i is one feature of the data point. Those points with similar features can then be grouped together and called a class, as in Figure 4.7. The second problem is deciding what the distinctive features of the data are and trying to keep this number as small as possible in order that the computer time and number of computations needed in the comparison process are kept to a minimum. The third problem is in deciding what form of decision-making process will be used for the comparison. Suppose that in the n-dimensional space there are M different classes each denoted by $g_1, g_2, \ldots, g_M$, the problem is deciding what the borders

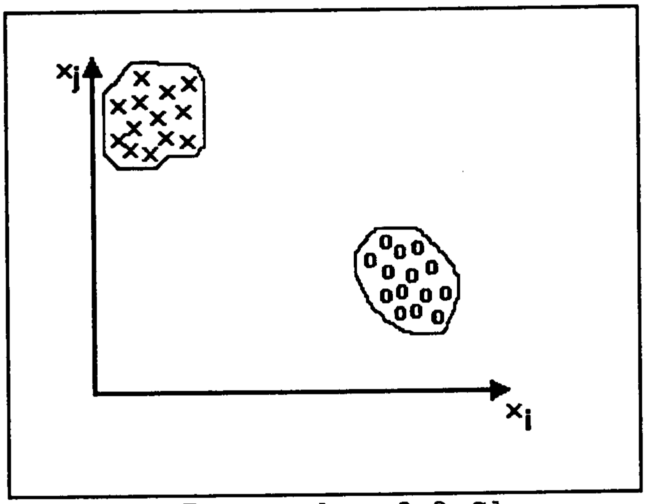

Figure 4.7 Sample of 2 Classes

of each class are. When unknown data are then entered they can be classified by which borders they lie within.

The use of distance functions is one of the most basic methods in classifying data, though it can only be effective if the different classes of data form clusters. In Figure 4.8, point **x** would be classified as belonging to class g_j, by using the nearest neighbor method. The *nearest neighbor* method can be defined as assigning "to an unclassified sample point the classification of the nearest of a set of previously classified points" (Cover, 1967). Using this method, **x**, an unknown point, would be allocated its closest neighbor's class s_i where

$$s_i \in \{s_1, s_2, \ldots, s_M\}$$

is the closest if

$$D(\boldsymbol{s_i}, \boldsymbol{x}) = \min_{l} D(\boldsymbol{s_l}, \boldsymbol{x}), \quad l = 1, 2, \ldots, N$$

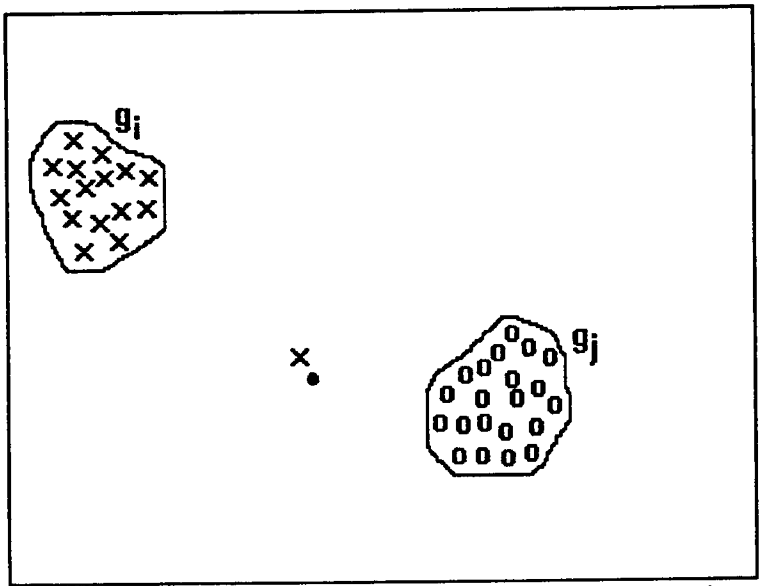

Figure 4.8 Example of Distance Function

and D is the distance measured. This method is the most effective when the number of samples is large, and has a probability error less than twice that of any other decision rule (Cover, 1967). If two classes are equally distant from the unknown point then another method will need to be used for its classification or it can be assigned to the class that has the greater population of the two. In the case of an axial-flow compressor, if the unknown point is halfway between normal operations and a rotating stall, a method like artificial neural networks or correlation matching might be used.

Correlation Matching

Another technique which can be used in the detection of some abnormality, like rotating stall or surge, is correlation matching. This procedure is another form of pattern recognition and is based on recognizing the linear association between a number of data sets (Bendat, 1980). Vectors are first formed from the data of the known patterns. An unknown pattern is then formed into a vector and the dot product of this vector and each of the other vectors are calculated. The results of these dot products, after being normalized, would produce a value near one if the data sets are similar and a value near zero if they are dissimilar.

This method was derived from a comparison between two n x 1 vectors *f* and *g*, one being the input and the other the reference.

$$m = \sum_{i=1}^{n} (f_i - g_i)^2$$

When *f* and *g* are identical *m* will be zero, and if greater than zero, then *f* and *g* are different. Expanding the squared term in the equation for *m* gives

$$m = \sum_{i=1}^{n} f_i^2 - 2\sum_{i=1}^{n} f_i g_i + \sum_{i=1}^{n} g_i^2.$$

From this it is easy to see that Σf_i^2 and Σg_i^2 are simply the squares of vector lengths, and are therefore inconsequential when comparing directions of the two vectors. $\Sigma f_i g_i$, though, yields the unnormalized correlation coefficient, c_{un}.

$$c_{un} = \sum_{i=1}^{n} f_i g_i$$

When c_{un} returns a large number, on account of Σfg being negative in the equation previous to this one, *m* will turn out to be small. This results in *m* showing how different *f* and *g* are, and c_{un} showing how close they are.

If either *f* or *g* have a component that is zero then this does nothing for the matching effort, especially if either one has a large number of zeros. In order to solve this, a normalized correlation is needed (Schalkoff, 1992).

$$c_n = \frac{\sum_{i=1}^{n} f_i \, g_i}{\sqrt{\sum_{i=1}^{n} f_i^2 * \sum_{i=1}^{n} g_i^2}}$$

A computer program was written for the calculation of the normalized correlation coefficient with the purpose of finding out whether or not it could aid in the detection of rotating stall in the axial-flow compressor of the 16 ft. transonic wind tunnel at AEDC. The program compared two data sets, *f* and *g*, checking to see if they were similar. An output close to the number one would mean that *f* was similar to *g*, and if it was close to zero then *f* would be dissimilar to *g*.

The program involved finding the unnormalized correlation coefficient (c_{un}) and dividing it by the normalizing value. The c_{un} was calculated by summing up the product of *f* and *g* at each of the amplitudes, corresponding to the selected frequencies. The normalizing value was determined by separately summing up the squares of *f* and *g*, and taking the square root of the products of these values.

The program was initially checked to see if it was working properly by comparing the sine and cosine values of a number moving from 0 to π. From this check the program was found to be working perfectly, giving a normalized correlation coefficient (c_n) of 0 at 0 and π, and a c_n of 1 at $\pi/4$.

Two different cases were checked, the first compared a sample of each blade with itself, the rest of the samples for that blade, and the three stall generated data sets for that blade, using just the amplitudes at the 16 selected frequencies (B.1 (a) - (f), located in Appendix B). The method worked pretty good, here. For patterns nearly identical, a correlation coefficient no lower than 0.91 was given. For patterns nearly opposite, a correlation coefficient no higher than 0.59 resulted.

In these tables, the first column is the unknown pattern and the second column is the known pattern. The third column contains the normalized correlation coefficient (c_n) which is the final result from the computer program when the vector formed by the data set of the pattern in the first column and the vector formed by the data set of the pattern in the second column are entered.

If two completely random vectors are used, a correlation coefficient close to 0.5 is expected. For the patterns that give a correlation coefficient of around 0.5, no final conclusion can be reached on whether or not the patterns can be associated with each other. Numbers near 1.0 would mean that the two vectors are extremely similar to each other, and numbers near 0.0 would indicate that the two vectors are nearly perpendicular and not similar.

The second case used the amplitudes of the entire frequency spectrum, all 201. It also compared a sample of each blade with itself, the rest of the samples for that blade, and the three stall generated data sets for that blade (B.2 (a) - (f), in Appendix B). There was an expectation that the correlation coefficient would not be as good as in the first case and this was proven true. This resulted from the fact that in the synthesized rotating stall data only the amplitudes at the major frequencies were adjusted and the rest of the amplitudes were left at their normal level. For the three similar samples the values ranged from a high of 1.0 to a low of almost 0.53. A correlation coefficient of 0.53 would be considered random.

When comparing the sample blade with the three stall generated data sets, the values range from a low of 0.19 to a high of 0.67. Since the patterns that are known to be similar have coefficients that are smaller than the patterns that are not similar, the second case would prove to be a failure.

The method was proven to work fairly well in the first case when just the relevant amplitudes were used. The patterns that were similar had correlation coefficients near 1.0. The patterns that were not similar had coefficients that sometimes stated that they weren't similar by being near 0.0 and other times they were near 0.5 which would have no clear meaning. For the second case in which all of the data was used, this method did work. The coefficients weren't as distinct as in the first case. Some of the similar patterns and dissimilar patterns gave random results, values near 0.5, from which no conclusion could be drawn.

A system that had data which contained some noise would affect this method. If it is minor then a fairly good correlation coefficient might result, but this method wouldn't be able to give good results if the system noise was significant.

A printout of the computer program used to calculate the normalized correlation coefficient can be found at the end of Appendix B.

Expert Systems

An expert system is a rule-based system built to solve problems in a specific area that requires reasoning, the ability to come to a conclusion, and to process information. It is formed from the knowledge of people who are considered to be experts in the required area. It could be used when the expert or experts are not always available to monitor and correct problems.

It consists of three elements: a knowledge base, rule base, and inference engines. The knowledge base is made up of a collection of facts about the specific area of interest, i.e. pressures, temperatures, stresses, valve positions, etc. Some of these facts are more important than others, like pressures may be more important than temperatures when it comes to rotating stall. To those facts which have a greater relevance to the problem larger weights are applied in order to show this greater importance. A rule base is a collection of IF...THEN rules that are used to apply the facts from the knowledge base to the particular situation. The rules, facts, and weights needed by the expert system are provided by an expert or group of experts who are very familiar with the situation. If an item or collection of items are true then there is an action to be taken. The inference engine can be considered the heart of the entire expert system. Its purpose is to match the facts from the knowledge base with the rules from the rule base, in order to make a decision.

The expert system has a number of advantages and disadvantages which must be realized before it can be used. They are able to give an explanation of their reasoning in reaching a particular answer. Expert systems don't require a large number of samples in order to be built. There are a large number of expert system computer programs available for the development of an expert system for a specific problem. Also, a sizeable number of expert systems exist which can be used for a reference. One of the disadvantages is that an expert in the specific area is needed for the construction of the system, which make take a large amount of time to develop. Unless properly organized the expert system may become unmanageable for large tasks (Caudill, 1991).

The object of the expert system is to achieve a goal. In the case of the detection of rotating stall or surge in an axial-flow compressor the goal could be the smooth operation of the compressor, or in the reverse case the detection of some form of unsteady phenomena. The facts for this system could come from a mix of pressure transducers, thermocouples, acoustic sensors, and strain gages. The inference engine might use a method called "backward chaining" to achieve the goal. It would start with the goal and find all of the THEN statements that would achieve this goal. Then the system would check the IFs of these THEN statements to see if they were true or false. If proven to be true, from the facts, the goal would be achieved. If, however, the condition of the IFs are unknown then the THENs answering these would be found and their IFs checked. This would continue backwards until everything is answered true or false, or if there were a few IFs left unanswered then these would be posed as questions to the user to answer. Once everything is answered, then the goal would be proven true or false.

For the example of detecting rotating stall or surge in a compressor, an expert system would not be the best answer because the data would be coming in real-time. The expert system works a little slower and wouldn't be able to check all of the incoming data. It's speed can be compared to the human operators. A better answer might be in the use of a neural network-based expert system. This is the combination of an expert system and a neural network. The neural network would be used for the real time monitoring of the compressor and when a rotating stall or surge was detected it would relay this to the expert system. This, in turn, would be able to help the compressor monitors to rectify the problem by informing them of all of their options. A neural network-based expert system has been shown to work in the case of the detection of stall in an axial compressor on the AEDC 16-foot transonic wind tunnel (Lo, June 1991).

The neural network part of the system would be able to do its calculations within a couple of seconds of receiving the data. The expert system if a rotating stall or surge is detected would immediately present this to the compressor operators along with its recommendations on corrective procedures. The entire process up until here will have taken approximately 15 - 20 seconds. If the artificial neural network comes up with an unknown, the expert system would have to try another method to resolve the unknown or present the compressor operators with a message that something is not right about the compressor and have them see if they can figure out what is happening. The complete process for this would take longer and could last anywhere from 30 seconds to several minutes.

CHAPTER 5

CONCLUSIONS AND RECOMMENDATIONS

The incorporation of artificial intelligence into monitoring systems is presently the only method that will speed up the detection of rotating stall and surge in axial-flow compressors that use one of the methods discussed in Chapter 3. If no method is currently used then, depending on the size of the compressor, thermocouples are the most promising stall/surge sensors for small compressors, and optical sensors for larger ones. The use of high response static pressure transducers show promise for detecting rotating stall at its inception but is still in its early stages of research and needs some more time.

Except for methods currently being researched, the only proven way of detecting rotating stall and surge is after they are fully developed. Therefore, the only way to save the axial compressor from possible damage is to detect these phenomena right after they start. Since the human operator doesn't have the time or the capability to watch over the compressors with enough detail, the computer must be used. Normal computer programs can not be used because the axial compressor is a fast-moving complex operating system which is used over a wide range of settings. As has been shown, a neural network has the capability to learn to recognize rotating stall and surge from normal operating conditions in real-time, in an axial-flow compressor. For interaction with the compressor operator an expert system could be used to recommend corrective actions upon detection of rotating stall or surge by a neural network.

If the neural network produces results which don't clearly indicate one way or another what is happening in the compressor, a back up method would be needed. Pattern recognition and correlation matching are two very good methods which could fill this role. They are simple to put together and use, given enough sample data. As has been shown, correlation matching can give pretty good results when used with the amplitudes of the primary frequencies. If an expert system receives an indication, from a neural network, that a rotating stall might be occurring in the axial compressor, it can use a technique like correlation matching to check the conclusion of the neural network.

Until the research is completed on prestall waves and their detection by high response static pressure transducers, the quickest way to detect rotating stall and surge is through something like a neural network-based expert system. With this, the task of closely watching axial-flow compressors would be eased. This system should detect a rotating stall or a surge within 20 seconds or so of its occurrence. This is easily within the time before a rotating stall would cause serious damage. A surge would probably be noticed by the operators about the same time the neural network-based expert system would notify them, unless a rotating stall preceded the surge.

Thermocouples are recommended for use in small axial compressors because of the generally even temperature distribution and the fact that they are proven and currently being used. Optical sensors are recommended for larger axial-flow compressors because they are easier to replace than strain gages, they provide coverage of the entire rotor stage, and they are easy to hook up.

BIBLIOGRAPHY

BIBLIOGRAPHY

Andrew, P.L., "A Computational Fluid Dynamic Method for Rotating Stall in a Single Stage Axial Compressor," The University of Tennessee, Knoxville, Tennessee, December 1985.

"Artificial Intelligence Tutor" (a computer program), Thinking Software, Inc., Woodside, NY, 1991.

Bendat, J.S., Piersol, A.G., Engineering Applications of Correlation and Spectral Analysis, John Wiley & Sons, Inc., New York, NY, 1980.

Bendat, J.S., Piersol, A.G., Random Data: Analysis and Measurement Procedures, Wiley-Interscience, New York, NY, 1971.

Binder, R.C., "A Study of Surging in Fan or Compressor Systems," Journal of the Franklin Institute, vol. 241, 1946, pp. 125-136.

Cargill, A.M., Freeman, C., "High-Speed Compressor Surge with Application to Active Control," Journal of Turbomachinery, April 1991, pp. 303-311.

Carter, A.D., Kilpatrick, D.A., "The Self-Excited Vibration of Axial-Flow Compressor Blades," Chartered Mechanical Engineers, November 1956, pp. 465-472.

Caudill, M., "Expert Networks," Byte, October 1991, pp. 108-116.

Caudill, M., Butler, C., Naturally Intelligent Systems, The MIT Press, Cambridge, MA, 1990.

Costilow, E.L., Huppert, M.C., "Rotating-Stall Characteristics of a Rotor with High Hub-Tip Radius Ratio," NACA TN-3518, 1955.

Cover, T.M., Hart, P.E., "Nearest Neighbor Pattern Classification", IEEE Transactions on Information Theory, January 1967, pp. 21-27.

Cover, T.M., "Estimation by the Nearest Neighbor Rule", IEEE Transactions on Information Theory, January 1968, pp. 50-55.

Cumpsty, N.A., Compressor Aerodynamics, John Wiley & Sons, Inc., New York, New York, 1989.

Daniel, T.W., "Detection, without Contact, of Rotor Blade Vibration in Axial Flow Compressors," The University of Tennessee, Knoxville, Tennessee, March 1968.

Daniel, T.W., "Stall Detection in Axial Flow Compressors," AEDC-TMR-79-G31, November 1979.

Das, D.K., Jiang, H.K., "An Experimental Study of Rotating Stall in a Multistage Axial-Flow Compressor," Journal of Engineering for Gas Turbines and Power, July 1984, pp. 542-551.

Das, D.K., Özcanli, S.C., "An Experimental Study of the Unsteady Response of the Rotor Blades of an Axial Flow Compressor Operating in the Rotating Stall Regime," AIAA Paper No. 83-0001, January, 1983.

Day, I.J., Greitzer, E.M., Cumpsty, N.A., "Prediction of Compressor Performance in Rotating Stall," Journal of Engineering for Power, January 1978, pp. 1-14.

Day, I.J., Cumpsty, N.A., "The Measurement and Interpretation of Flow within Rotating Stall Cells in Axial Compressors," Journal Mechanical Engineering Sciences, April 1978, pp. 101-114.

Duke, J.L., "Use of a Deliberate Nonlinearity to Improve the Performance of an Axial Flow Compressor Surge Control System," The University of Tennessee, Knoxville, Tennessee, June 1962.

Dundas, R.E., "The Use of Performance-Monitoring to Prevent Compressor and Turbine Blade Failures," ASME Paper No. 82-GT-66, April 1982.

Emmons, H.W., Pearson, C.E., Grant, H.P., "Compressor Surge and Stall Propagation," Transactions of the ASME, April 1955, pp. 455-469.

Fabri, J., "Rotating Stall in Axial Compressors," NASA TT F-11, 765, December 1968.

Forney, L.J., "Frequency Response of a Thermocouple Wire: Effects of Axial Conduction," Progress Report, April 1990 - September 1990, NASA-CR-180454.

Forney, L.J., Meeks, E.L., Fralick, G.C., "Frequency Response of a Supported Thermocouple Wire: Effects of

Axial Conduction," Progress Report, October 1990 - March 1991, NASA-CR-188101.

Fowler, M.D., "Quantitative Evaluation of the Effects of Transient Heat Transfer on Axial Flow Compressor Stability," The University of Tennessee, Knoxville, Tennessee, December 1984.

Folwer, R.B., "Online Monitoring of Compressor Blade Stress: An Improved System," AEDC-TR-79-7, April 1979.

Gamache, R.N., Greitzer, E.M., "Reverse Flow in Multistage Axial Compressors," Journal of Propulsion and Power, July-August 1990, pp. 461-473.

Garnier, V.H., Epstein, A.H., Greitzer, E.M., "Rotating Waves as a Stall Inception Indication in Axial Compressors," Journal of Turbomachinery, April 1991, pp. 290-302.

Golden, J., "A Neural Network for the Analysis of Test Data from the Aeropropulsion Systems Test Facility," The University of Tennessee, Knoxville, Tennessee, August 1990.

Gostelow, J.P., Cascade Aerodynamics, Pergamon Press, New York, NY, 1984.

Greitzer, E.M., "Surge and Rotating Stall in Axial Flow Compressors - Part I: Theoretical Compression System Model," Journal of Engineering for Power, April 1976, pp. 190-198.

Greitzer, E.M., "Surge and Rotating Stall in Axial Flow Compressors - Part II: Experimental Results and Comparison with Theory," Journal of Engineering for Power, April 1976, pp. 199-217.

Greitzer, E.M., "REVIEW - Axial Compressor Stall Phenomena," Journal of Fluids Engineering, June 1980, pp. 134-151.

Hamrick, J.T., "The Surge Problem as Related to the ASME Compressor Test Code PTC 10-1949", Presented at the Joint Conference of the ASME Gas Turbine Power and Hydraulic Divisions, Houston, Texas, March 6-9, 1960.

Hawthorne, W.R., edt., Aerodynamics of Turbines and Compressors, Princeton University Press, Princeton, New Jersey, 1964.

Hecht-Nielsen, R., Neurocomputing, Addison-Wesley Publishing Company, Reading, MA, 1990.

Hohenberg, R., "Detection and Study of Compressor-blade Vibration," Experimental Mechanics, June 1967, pp. 19A-24A.

Horlock, J.H., Axial Flow Compressors, Butterworths Scientific Publications, London, 1958.

Huppert, M.C., Benser, W.A., "Some Stall and Surge Phenomena in Axial-Flow Compressors", Journal of the Aeronautical Sciences, December 1953, pp. 835-845.

Inoue, M., Kuroumaru, M., Iwamoto, T., Ando, Y., "Detection of a Rotating Stall Precursor in Isolated Axial Flow Compressor Rotors," Journal of Turbomachinery, April 1991, pp. 281-289.

Jackson, A.D., "Stall Cell Development in an Axial Compressor," Journal of Turbomachinery, October 1987, pp. 492-498.

Jenny, R., Gremli, C., Gumoes, H.B., "Practical Experience with a Non-Contact Blade Vibration Measuring System in Industrial Turbocompressors," Aeroelasticity in Turbomachines, Proceedings of the Second International Symposium, Lausanne, Switzerland, September 8-12, 1980, pp. 419-428.

Johnsen, I.A., Bullock, R.O., eds., Aerodynamic Design of Axial Flow Compressors, NASA SP-36, 1965.

Klimasauskas, C.C., "Apply Neural Networks - Part 1: An Overview of the Series," PC AI, January/February 1991, pp. 30-33.

Laurence, J.C., Landes, L.G., "Auxiliary Equipment and Techniques for Adapting the Constant-Temperature Hot-wire Anemometer to Specific Problems in Air-flow Measurements," NACA TN 2843, November 1952.

Leiblein, S., Lewis, G.W., Jr., Sandercock, D.M., "Experimental Investigation of an Axial-Flow Compressor Inlet Stage Operating at Transonic Relative Inlet Mach Numbers. I - Overall Performance of Stage with Transonic Rotor and Subsonic Stators Up to Rotor Relative Inlet Mach Number of 1.1," NACA RM E52A24, 1952.

Leiblein, S., Schwenk, F.C., Broderick, R.L., "Diffusion Factor for Estimating Losses and Limiting Blade Loadings in Axial-Flow Compressor Blade Elements," NACA RM E53D01, 1953.

Levine, R.I., Drang, D.E., Edelson, B., AI and Expert Systems, McGraw-Hill Publishing Company, New York, NY, 1990.

Liu, W., "An Expert System for Predicting Flutter in Turbomachines," AIAA Paper No. 91-2527, June 1991.

Lo, C.F., "Engineering Monitoring Expert System's Developer," Final Report, NAG2-596 & NAG2-596 Supplement 1, February 1991.

Lo, C.F., Shi, G.Z., "Neural Network Based Expert System for Compressor Stall Monitoring," AIAA Paper No. 91-2500, June 1991.

Maren, A.J., Harston, C.T., Pap, R.M., Handbook of Neural Computing Applications, Academic Press, Inc., San Diego, CA, 1990.

Mazzawy, R.S., "Surge-Induced Structural Loads in Gas Turbines," Journal of Engineering for Power, January 1990, pp. 162-168.

McDougall, N.M., "A Comparison Between the Design Point and Near-Stall Performance of an Axial Compressor," Journal of Turbomachinery, January 1990, pp. 109-115.

McDougall, N.M., Cumpsty, N.A., Hynes, T.P., "Stall Inception in Axial Compressors," Journal of Turbomachinery, January 1990, pp. 116-125.

Mikolajczak, A.A., Arnoldi, R.A., Snyder, L.E., Stargardter, H., "Advances in Fan and Compressor Blade Flutter Analysis and Predictions," Journal of Aircraft, April 1975, pp. 325-332.

Moore, F.K., "A Theory of Rotating Stall of Multistage Axial Compressors: Part I - Small Disturbances," Journal of Engineering for Gas Turbines and Power, April 1984, pp. 313-320.

Moore, F.K., "A Theory of Rotating Stall of Multistage Axial Compressors: Part II - Finite Disturbances," Journal of Engineering for Gas Turbines and Power, April 1984, pp. 321-326.

Moore, F.K., "A Theory of Rotating Stall of Multistage Axial Compressors: Part III - Limit Cycles," Journal of Engineering for Gas Turbines and Power, April 1984, pp. 327-336.

NeuralWorks Explorer (a computer program), NeuralWare, Inc., 1988.

Nieberding, W.C., Pollack, J.L., "Optical Detection of Blade Flutter," NASA TM X-73573, 1977.

Nolen, T., "The Intelligent Application of AI Tools," PC AI, January/February 1991, pp. 24-27.

Oates, G.C., Aerothermodynamics of Gas Turbine and Rocket Propulsion, American Institute of Aeronautics and Astronautics, Washington, D.C., 1988.

Parker, R., "An Investigation of Acoustic Resonance Effects in an Axial Flow Compressor Stage," Journal of Sound and Vibration, 1968, pp. 281-297.

Parker, R., "Acoustic Resonances and Blade Vibration in Axial Flow Compressors," Journal of Sound and Vibration, February 1984, pp. 529-539.

Pearson, C.E., "A Study of Surge in Compressors and Jet Engines," Journal of the Aeronautical Sciences, January 1955, pp. 10-16.

Pearson, C.E., "Surge Behavior in a Three-Stage Compressor," Journal of the Aeronautical Sciences, November 1955, pp. 799-802.

Province, G.T., "A Microprocessor-Controlled System for Real Time Signature Analysis," The University of Tennessee, Knoxville, Tennessee, December 1979.

Ruden, P., "Investigation of Single Stage Axial Fans," NACA TM 1062, 1944.

Schäffler, A., Miatt, D.C., "Experimental Evaluation of Heavy Fan - High-Pressure Compressor Interaction in a Three-Shaft Engine: Part 1 - Experimental Setup and Results," Journal of Engineering for Gas Turbines and Power, October 1985, pp. 828-832.

Schalkoff, R.J., Pattern Recognition: Statistical, Structural, and Neural Approaches, John Wiley & Sons, Inc., New York, NY, 1992.

Stenning, A.H., "Rotating Stall and Surge," Journal of Fluids Engineering, March 1980, pp. 14-20.

Taylor, E.S., "Evolution of the Jet Engine," Astronautics and Aeronautics, November 1970, pp. 64-72.

Tou, J.T., Gonzalez, R.C., Pattern Recognition Principles, Addison-Wesley Publishing Company, Reading, Massachusetts, 1974.

Wasserman, P.D., Neural Computing Theory and Practice, Van Nostrand Reinhold, New York, NY, 1989.

Womack, R., Engineer, Calspan Corporation, Personal Interview, July 15, 1991.

APPENDIXES

APPENDIX A

SAMPLE DATA

Table A.1 Strain Gage Data from Axial Compressor

Sensors	6.5 Hz	10.0 Hz	12.5 Hz	15.0 Hz
A13-01	360.05	2515.02	492.27	964.65
A13-02	486.74	3159.40	932.76	660.93
A13-03	228.32	2529.28	840.30	848.71
B01-01	86.22	768.97	486.64	485.44
B01-02	282.66	1147.83	388.51	544.07
B01-03	206.42	1278.71	158.81	273.33
C16-01	248.07	544.98	396.71	593.26
C16-02	242.82	970.84	261.39	490.45
C16-03	1104.70	2394.73	3223.30	3254.80
A13-S1	14402.13	2515.02	5907.22	964.65
A13-S2	19469.43	3159.40	11193.15	660.93
A13-S3	9132.94	2529.28	10083.58	848.71
B01-S1	3448.90	768.97	5839.74	485.44
B01-S2	11306.55	1147.83	4662.14	544.07
B01-S3	8256.87	1278.71	1905.72	237.33
C16-S1	9922.72	544.98	4760.57	593.26
C16-S2	9712.87	970.84	3136.72	490.45
C16-S3	44187.86	2394.73	38679.64	3254.80

Table A.1 (continued)

Sensors	20.0 Hz	25.0 Hz	27.5 Hz	30.0 Hz
A13-01	6893.44	1610.49	4745.27	13993.75
A13-02	7322.80	2431.92	4856.49	16057.60
A13-03	6104.03	3838.15	6815.25	14391.47
B01-01	3252.03	599.78	1759.87	9540.18
B01-02	6203.17	576.30	2409.95	14171.67
B01-03	6320.43	1078.10	1489.63	9710.22
C16-01	3943.34	3238.58	4329.91	20094.61
C16-02	3998.01	837.73	4124.01	20218.13
C16-03	4979.50	2385.89	3004.35	16524.91
A13-S1	6893.44	6441.94	15690.00	5597.50
A13-S2	7322.80	9727.68	12201.92	6423.04
A13-S3	6104.03	15352.58	10355.86	5756.59
B01-S1	3252.03	2399.11	7039.48	3816.07
B01-S2	6203.17	2305.21	6128.01	5668.67
B01-S3	6320.43	4312.40	5656.10	3884.09
C16-S1	3943.34	12954.32	17319.63	8037.84
C16-S2	3998.01	3308.46	14710.25	8087.25
C16-S3	4979.50	9543.56	9741.31	6609.96

Table A.1 (continued)

Sensors	35.0 Hz	40.0 Hz	45.0 Hz	50.0 Hz
A13-01	2248.32	5556.99	773.31	3073.44
A13-02	1570.21	5031.62	931.73	1669.94
A13-03	2027.60	5346.46	1185.40	2297.51
B01-01	973.46	398.20	458.97	2349.05
B01-02	1777.84	2266.30	506.32	3427.65
B01-03	1531.21	1668.47	861.53	2672.88
C16-01	1641.33	3971.98	874.22	1761.33
C16-02	1525.50	4708.07	1107.18	1111.41
C16-03	1009.89	3362.11	827.90	1036.55
A13-S1	2248.32	2778.50	773.31	3073.44
A13-S2	1570.21	2515.81	931.73	1669.94
A13-S3	2027.60	2673.23	1185.40	2297.51
B01-S1	973.46	199.10	458.97	2349.05
B01-S2	1777.84	1133.15	506.32	3427.65
B01-S3	1531.21	834.24	861.53	2672.88
C16-S1	1641.33	1985.99	874.22	1761.33
C16-S2	1525.50	2354.03	1107.18	1111.41
C16-S3	1009.89	1681.06	827.90	1036.55

Table A.1 (continued)

Sensors	70.0 Hz	74.0 Hz	80.0 Hz	90.0 Hz
A13-01	39591.49	4068.24	6463.06	8221.64
A13-02	21012.91	4721.57	3985.62	7890.59
A13-03	21016.54	7863.34	5167.33	10685.91
B01-01	14915.44	6440.75	1888.80	1625.13
B01-02	18931.22	2773.52	3435.71	3215.64
B01-03	26434.97	6503.60	3605.34	5135.34
C16-01	10697.50	1333.02	2836.87	6964.25
C16-02	15505.42	3169.34	4535.09	6734.48
C16-03	8328.65	2008.36	2809.60	5900.14
A13-S1	6598.58	16272.97	4308.71	4110.82
A13-S2	3502.15	18886.29	2657.08	3945.29
A13-S3	3502.76	31453.37	3444.89	5329.46
B01-S1	2485.91	25762.99	1259.20	812.56
B01-S2	3155.20	11094.06	2290.47	1607.82
B01-S3	4405.83	26014.42	2403.56	2567.67
C16-S1	1782.92	5332.09	1891.24	3482.12
C16-S2	2584.24	12677.34	3023.39	3367.24
C16-S3	1388.11	8033.42	1873.06	2950.07

Table A.2 Normalized Strain Gage Data

Sensors	6.5 Hz	10.0 Hz	12.5 Hz	15.0 Hz
A13-01	0.006209	0.753527	0.008657	0.231872
A13-02	0.009082	1.000000	0.020092	0.130005
A13-03	0.003222	0.758983	0.017691	0.192986
B01-01	0.000000	0.085675	0.008511	0.071144
B01-02	0.004454	0.230589	0.005963	0.090807
B01-03	0.002726	0.280647	0.000000	0.000000
C16-01	0.003670	0.000000	0.006176	0.107308
C16-02	0.003551	0.162890	0.002663	0.072824
C16-03	0.023094	0.707519	0.079554	1.000000
A13-S1	0.324612	0.753527	0.149229	0.231872
A13-S2	0.439512	1.000000	0.286451	0.130005
A13-S3	0.205133	0.758983	0.257647	0.192986
B01-S1	0.076248	0.085675	0.147477	0.071144
B01-S2	0.254420	0.230589	0.116906	0.090807
B01-S3	0.185269	0.280647	0.045350	0.000000
C16-S1	0.223041	0.000000	0.119462	0.107308
C16-S2	0.218283	0.162890	0.077306	0.072824
C16-S3	1.000000	0.707519	1.000000	1.000000

Table A.2 (continued)

Sensors	20.0 Hz	25.0 Hz	27.5 Hz	30.0 Hz
A13-01	0.932094	0.069989	0.229495	0.676119
A13-02	1.000000	0.125581	0.236310	0.783510
A13-03	0.807243	0.220749	0.356335	0.696814
B01-01	0.356176	0.001589	0.046562	0.444381
B01-02	0.822923	0.000000	0.086396	0.685377
B01-03	0.841468	0.033960	0.030003	0.453229
C16-01	0.465513	0.180172	0.204043	0.993573
C16-02	0.474159	0.017693	0.191427	1.000000
C16-03	0.629389	0.122466	0.122818	0.807826
A13-S1	0.932094	0.396963	0.900143	0.239227
A13-S2	1.000000	0.619329	0.686408	0.282184
A13-S3	0.807243	1.000000	0.573289	0.247505
B01-S1	0.356176	0.123360	0.370075	0.146532
B01-S2	0.822923	0.117006	0.314224	0.242930
B01-S3	0.841468	0.252844	0.285307	0.150071
C16-S1	0.465513	0.837695	1.000000	0.366209
C16-S2	0.474159	0.184902	0.840108	0.368779
C16-S3	0.629389	0.606868	0.535632	0.291910

Table A.2 (continued)

Sensors	35.0 Hz	40.0 Hz	45.0 Hz	50.0 Hz
A13-01	1.000000	1.000000	0.432725	0.854091
A13-02	0.468094	0.901945	0.650798	0.275963
A13-03	0.826872	0.960707	1.000000	0.534473
B01-01	0.000000	0.037160	0.000000	0.555701
B01-02	0.630957	0.385823	0.065192	1.000000
B01-03	0.437503	0.274245	0.554163	0.689092
C16-01	0.523882	0.704173	0.571634	0.313607
C16-02	0.433024	0.841556	0.892318	0.045891
C16-03	0.028577	0.590347	0.507866	0.015057
A13-S1	1.000000	0.481420	0.432725	0.854091
A13-S2	0.468094	0.432393	0.650798	0.275963
A13-S3	0.826872	0.461774	1.000000	0.534473
B01-S1	0.000000	0.000000	0.000000	0.555701
B01-S2	0.630957	0.174331	0.065192	1.000000
B01-S3	0.437503	0.118543	0.554163	0.689092
C16-S1	0.523882	0.333506	0.571634	0.313607
C16-S2	0.433024	0.402198	0.892318	0.045891
C16-S3	0.028577	0.276594	0.507866	0.015057

Table A.2 (continued)

Sensors	70.0 Hz	74.0 Hz	80.0 Hz	90.0 Hz
A13-01	1.000000	0.100752	1.000000	0.752469
A13-02	0.518584	0.122206	0.546510	0.718848
A13-03	0.518678	0.225372	0.762819	1.000000
B01-01	0.360583	0.178658	0.162692	0.082524
B01-02	0.464642	0.058237	0.445851	0.244057
B01-03	0.659082	0.180722	0.476901	0.439023
C16-01	0.251286	0.010935	0.336234	0.624768
C16-02	0.375871	0.071235	0.647089	0.601433
C16-03	0.189903	0.033111	0.331242	0.516697
A13-S1	0.145073	0.501520	0.605651	0.334972
A13-S2	0.064837	0.587334	0.303324	0.318162
A13-S3	0.064853	1.000000	0.447530	0.458738
B01-S1	0.038503	0.813145	0.047446	0.000000
B01-S2	0.055847	0.331460	0.236218	0.080766
B01-S3	0.088253	0.821401	0.256918	0.178249
C16-S1	0.020287	0.142253	0.163140	0.271122
C16-S2	0.041051	0.383450	0.370377	0.259454
C16-S3	0.010057	0.230957	0.159812	0.217086

APPENDIX B

CORRELATION MATCHING RESULTS

B.1 (a) C_n Comparing a Sample of Blade A13 with Normal and Stall Samples Using the 16 Selected Amplitudes

f	g	C_n
A13-01	A13-01	1.0000
A13-01	A13-02	0.9447
A13-01	A13-03	0.9292
A13-01	A13-S1	0.4588
A13-01	A13-S2	0.3289
A13-01	A13-S3	0.3122

B.1 (b) C_n Comparing a Sample of Blade A17 with Normal and Stall Samples Using the 16 Selected Amplitudes

f	g	C_n
A17-01	A17-01	1.0000
A17-01	A17-02	0.9711
A17-01	A17-03	0.9956
A17-01	A17-S1	0.5007
A17-01	A17-S2	0.5301
A17-01	A17-S3	0.5320

B.1 (c) C_n Comparing a Sample of Blade B01 with Normal and Stall Samples Using the 16 Selected Amplitudes

f	g	C_n
B01-01	B01-01	1.0000
B01-01	B01-02	0.9659
B01-01	B01-03	0.9665
B01-01	B01-S1	0.5007
B01-01	B01-S2	0.5639
B01-01	B01-S3	0.5511

B.1 (d) C_n Comparing a Sample of Blade B02 with Normal and Stall Samples Using the 16 Selected Amplitudes

f	g	C_n
B02-01	B02-01	1.0000
B02-01	B02-02	0.9787
B02-01	B02-03	0.9907
B02-01	B02-S1	0.4951
B02-01	B02-S2	0.4716
B02-01	B02-S3	0.4555

B.1 (e) C_n Comparing a Sample of Blade C16 with Normal and Stall Samples Using the 16 Selected Amplitudes

f	g	C_n
C16-01	C16-01	1.0000
C16-01	C16-02	0.9794
C16-01	C16-03	0.9724
C16-01	C16-S1	0.5392
C16-01	C16-S2	0.5548
C16-01	C16-S3	0.2027

B.1 (f) C_n Comparing a Sample of Blade C17 with Normal and Stall Samples Using the 16 Selected Amplitudes

f	g	C_n
C17-01	C17-01	1.0000
C17-01	C17-02	0.9822
C17-01	C17-03	0.9947
C17-01	C17-S1	0.4951
C17-01	C17-S2	0.5227
C17-01	C17-S3	0.5896

B.2 (a) C_n Comparing a Sample of Blade A13 with Normal and Stall Samples Using all of the Amplitudes

f	g	C_n
A13-01	A13-01	1.0000
A13-01	A13-02	0.7597
A13-01	A13-03	0.8811
A13-01	A13-S1	0.6496
A13-01	A13-S2	0.3523
A13-01	A13-S3	0.3402

B.2 (b) C_n Comparing a Sample of Blade A17 with Normal and Stall Samples Using all of the Amplitudes

f	g	C_n
A17-01	A17-01	1.0000
A17-01	A17-02	0.7912
A17-01	A17-03	0.9348
A17-01	A17-S1	0.6643
A17-01	A17-S2	0.5221
A17-01	A17-S3	0.6044

B.2 (c) C_n Comparing a Sample of Blade B01 with Normal and Stall Samples Using all of the Amplitudes

f	g	C_n
B01-01	B01-01	1.0000
B01-01	B01-02	0.7713
B01-01	B01-03	0.8076
B01-01	B01-S1	0.5488
B01-01	B01-S2	0.3963
B01-01	B01-S3	0.4095

B.2 (d) C_n Comparing a Sample of Blade B02 with Normal and Stall Samples Using all of the Amplitudes

f	g	C_n
B02-01	B02-01	1.0000
B02-01	B02-02	0.9164
B02-01	B02-03	0.9221
B02-01	B02-S1	0.5798
B02-01	B02-S2	0.4772
B02-01	B02-S3	0.4643

B.2 (e) C_n Comparing a Sample of Blade C16 with Normal and Stall Samples Using all of the Amplitudes

f	g	C_n
C16-01	C16-01	1.0000
C16-01	C16-02	0.9431
C16-01	C16-03	0.8888
C16-01	C16-S1	0.5094
C16-01	C16-S2	0.5015
C16-01	C16-S3	0.1965

B.2 (f) C_n Comparing a Sample of Blade C17 with Normal and Stall Samples Using all of the Amplitudes

f	g	C_n
C17-01	C17-01	1.0000
C17-01	C17-02	0.5344
C17-01	C17-03	0.9423
C17-01	C17-S1	0.5731
C17-01	C17-S2	0.4328
C17-01	C17-S3	0.5857

```
c*********************************************************
c
c       A program to calculate the normalized correlation
c       coefficient
c
c                       by  John Sebghati
c
c*********************************************************
c
c       definition of variables:
c
c       cn   = normalized correlation coefficient
c       e    = normalizing value
c       f    = reference vector
c       fg   = sum of the reference vectors multiplied by
c              the input vectors
c       g    = input vector
c       i    = do-loop variable
c       n    = number of components in vector
c       sumf = sum of reference vectors squared
c       sumg = sum of input vectors squared
c
c*********************************************************

      double precision f(16),g(16),sumf,sumg,e,fg,cn

      open(unit=6,file='fdata.dat',status='old')
      open(unit=7,file='gdata.dat',status='old')

c*********************************************************
c
c       Constants
c
c*********************************************************

      n = 16
      sumf = 0.0
      sumg = 0.0
      fg = 0.0

c*********************************************************
c
c       Input
c
c*********************************************************

      do 10 i = 1,n

         read(6,*) f(i)
         read(7,*) g(i)

 10   continue
```

```
c***********************************************************
c
c       Calculate Sum of Squared Vectors
c
c***********************************************************

      do 20 i = 1,n

         sumf = sumf + f(i)**2.0
         sumg = sumg + g(i)**2.0

 20   continue

c***********************************************************
c
c       Calculate Normalizing Value
c
c***********************************************************

      e = dsqrt(sumf * sumg)

c***********************************************************
c
c       Calculate Unnormalized Correlation Coefficient
c
c***********************************************************

      do 30 i = 1,n

         fg = fg + f(i) * g(i)

 30   continue

c***********************************************************
c
c       Calculate Normalized Correlation Coefficient
c
c***********************************************************

      cn = fg / e

c***********************************************************
c
c       Output
c
c***********************************************************

      print *,'cn = ',cn


      stop
      end
```

VITA

John Michael Sebghati was born October 14, 1965 in Winnipeg, Canada. He attended elementary school and junior high school in Council Bluffs, Iowa, and graduated from Creighton Preparatory School in Omaha, Nebraska, in 1984. He received a Bachelor of Science Degree in Aerospace Engineering from Iowa State University, Ames, Iowa in 1989, and started at The University of Tennessee Space Institute, Tullahoma, Tennessee, in January 1990, where he pursued a Master of Science Degree in Aerospace Engineering.

He was awarded the rank of Eagle Scout in October 1982. In April 1991, he was the chairperson of the 1991 American Institute of Aeronautics and Astronautics (AIAA) Southeast Regional Student Conference in Orlando, Florida, and has been a member of the AIAA since 1986.